Chapter 9

Methods to Monitor Mitophagy and Mitochondrial Quality: Implications in Cancer, Neurodegeneration, and Cardiovascular Diseases

Simone Patergnani, Massimo Bonora, Esmaa Bouhamida, Alberto Danese, Saverio Marchi, Giampaolo Morciano, Maurizio Previati, Gaia Pedriali, Alessandro Rimessi, Gabriele Anania, Carlotta Giorgi, and Paolo Pinton

Abstract

Mitochondria are dynamic organelles that participate in a broad array of molecular functions within the cell. They are responsible for maintaining the appropriate energetic levels and control the cellular homeostasis throughout the generation of intermediary metabolites. Preserving a healthy and functional mitochondrial population is of fundamental importance throughout the life of the cells under pathophysiological conditions. Hence, cells have evolved fine-tuned mechanisms of quality control that help to preserve the right amount of functional mitochondria to meet the demand of the cell. The specific recycling of mitochondria by autophagy, termed mitophagy, represents the primary contributor to mitochondrial quality control. During this process, damaged or unnecessary mitochondria are recognized and selectively degraded. In the past few years, the knowledge in mitophagy has seen rapid progress, and a growing body of evidence confirms that mitophagy holds a central role in controlling cellular functions and the progression of various human diseases.

In this chapter, we will discuss the pathophysiological roles of mitophagy and provide a general overview of the current methods used to monitor and quantify mitophagy. We will also outline the main established approaches to investigate the mitochondrial function, metabolism, morphology, and protein damage.

Key words Metabolism, Mitochondrial morphology, Pathology, Mitochondrial quality control, Cardiovascular diseases (CVD), Homeostasis

1 Introduction

The functions attributed to the mitochondria among the more general cellular activities have been progressively increasing during the last decades, strongly changing the textbook image of an intracellular organelle, principally seen as an energy provider. A more precise draw has to consider mitochondria as pivotal regulators of

Carlos M. Palmeira and Anabela P. Rolo (eds.), *Mitochondrial Regulation: Methods and Protocols*, Methods in Molecular Biology, vol. 2310, https://doi.org/10.1007/978-1-0716-1433-4_9,

cell death, being it able to respond to different death stimuli through the release of mitochondrial proteins able to trigger the proapoptotic routine. Presence of specialized zones, where mitochondria contact the endoplasmic reticulum (ER), allows for a regulated exchange of lipids, cholesterol, and in particular, Calcium (Ca^{2+}) [1–4], whose influx and outflow influence both mitochondrial enzymatic activities or specialized cytoplasmic functions like muscle contraction and others. The outer mitochondrial membrane (OMM) behaves as a dock surface for several proteins involved in the inflammatory and antiviral response [5], and, in addition, the release of mitochondrial(mt)DNA and formyl peptides from mitochondria, both intra or extracellularly, strongly prompts the inflammatory response. Mitochondria are not only providers of adenosine triphosphate (ATP), but also generators of metabolic intermediates to be used for the synthesis of fatty acids and amino acids and are so flexible to switch among these different functions to meet the cellular requirements. Mitochondria are also the source of iron-sulfur clusters, which are present in a wide number of mitochondrial and not mitochondrial proteins [6]. Being mitochondria as regulatory platforms of different cellular functions is not surprising that not only their specific functions, but also their number and the quality of their activities have to be strictly regulated. Mitochondria usually are present in the cells under the form of a dynamic network, where mitochondrial mass increases as a consequence of mitochondrial biogenesis, while its diminution can occur through a selective form of autophagy, termed mitophagy. Autophagy is a more general mechanism that is devised to destroy and recycle intracellular organelles, parts of cytoplasm and unfolded or aggregated proteins, lipid droplets, and xenobiotics. Although being important to recycle metabolic intermediate and fuel cell metabolism under shortage conditions, the autophagic process itself is something more than a mere degradative process. Instead, it is devised to reshape the cellular composition, often eliminating, selectively, the damaged or nonfunctional part of the cell. Autophagy is under the control of the regulatory kinases mechanistic target of rapamycin (mTOR) and 5′ adenosine monophosphate-activated protein (AMPK). mTOR exerts a general inhibitory drive on autophagy, and its activity is reduced when the overall metabolic demand exceeds the supply. On the contrary, AMPK promotes autophagy, and it can be activated by impairment of mitochondrial activity, in terms of lesser ATP synthesis, reduced oxygen (O_2) consumption, increased reactive oxygen species (ROS) production, or Ca^{2+} mobilization [7].

Mitophagy regulation is not a completely clarified topic yet. During short-term starvation, mitochondrial pool is not depleted, to not further reduce cellular production of energy, while general autophagy can occur to sustain oxidative metabolism [8]. Prolonged starvation can lead to mitochondrial depletion through a nonspecific mechanism that can also involve other organelles and

cytoplasm. On the contrary, mitochondrial ROS production or depolarization can trigger mitophagy machinery, which is organized into different moments: the identification of the parts of the mitochondrial network to address to demolition and the recruitment to the autophagic machinery, which terminates with fusion to lysosomes.

There are several mechanisms by which mitophagy is induced. The first observation concerned reticulocytes that, during differentiation, loss mitochondria by mitophagy throughout the activity of NIP3-like protein X (NIX/BNIP3L). Another mechanism was found upon hypoxic conditions, where the OMM protein FUNDC1 works as a mitophagic receptors, thanks to its microtubule-associated proteins 1A/1B light chain 3B (LC3)-binding domain at N-terminal level [9]. Similarly, FK506-binding protein 8 (FKBP8) and BCL2L13 were identified as a LC3-interacting proteins capable to activate mitophagy [10, 11]. Undoubtedly, the most studied is the molecular mechanism regulated by the PTEN-induced kinase 1 (PINK1)/Parkin axis. PINK1 and Parkin belong to a series of genes referred to as PARK genes. Mutations in these genes (α-synuclein (α-syn, PARK1/4), parkin (PARK2), PINK1 (PTEN-Induced Kinase 1—PARK6), DJ-1 (PARK7), LRRK2 (PARK8), and ATP13A2 (PARK9)) have been linked to familiar forms of Parkinson's disease (PD). Studies occurring in these PD forms have permitted to provide insight into the molecular mechanisms of mitophagy. In particular, it has been demonstrated that PINK1 and Parkin act in a common pathway to regulate mitochondrial function, autophagy, and protein accumulation. From its discovery in 1998, about 100 mutations have been identified for Parkin gene as a causative gene for autosomal recessive parkinsonism [12]. The Parkin gene product is a cytosolic protein characterized by an ubiquitin-like (UBL) domain at the N-terminus.

Originally linked to autosomal recessive early-onset PD in 2004, PINK1 encodes a ubiquitous protein characterized by a mitochondrial targeting sequence (MTS), a transmembrane domain, and a highly conserved serine/threonine kinase domain. At today, about 30 pathogenic PINK1 mutations have been identified to impair its kinase activity and provoke loss of function [13–15]. Normally, the levels of PINK1 are very low. This is due to a fine-tuned mechanism that begins with the import of PINK1 into mitochondria by the activity of the translocases of the inner (TIM23) and outer (TOM) membrane complex (Fig. 1). Once arrived in the inner mitochondrial membrane (IMM), PINK1 is subjected to series of proteolytic cleavages that reduce the full-length form of PINK1 into fragments, which are then degraded by proteasome [16–18]. When stress conditions increase and mitochondria suffer damages, the activity of TIM23/TOM complex is disrupted, and PINK1 accumulates on the OMM. Here, once stabilized by a molecular complex composed of TOM proteins

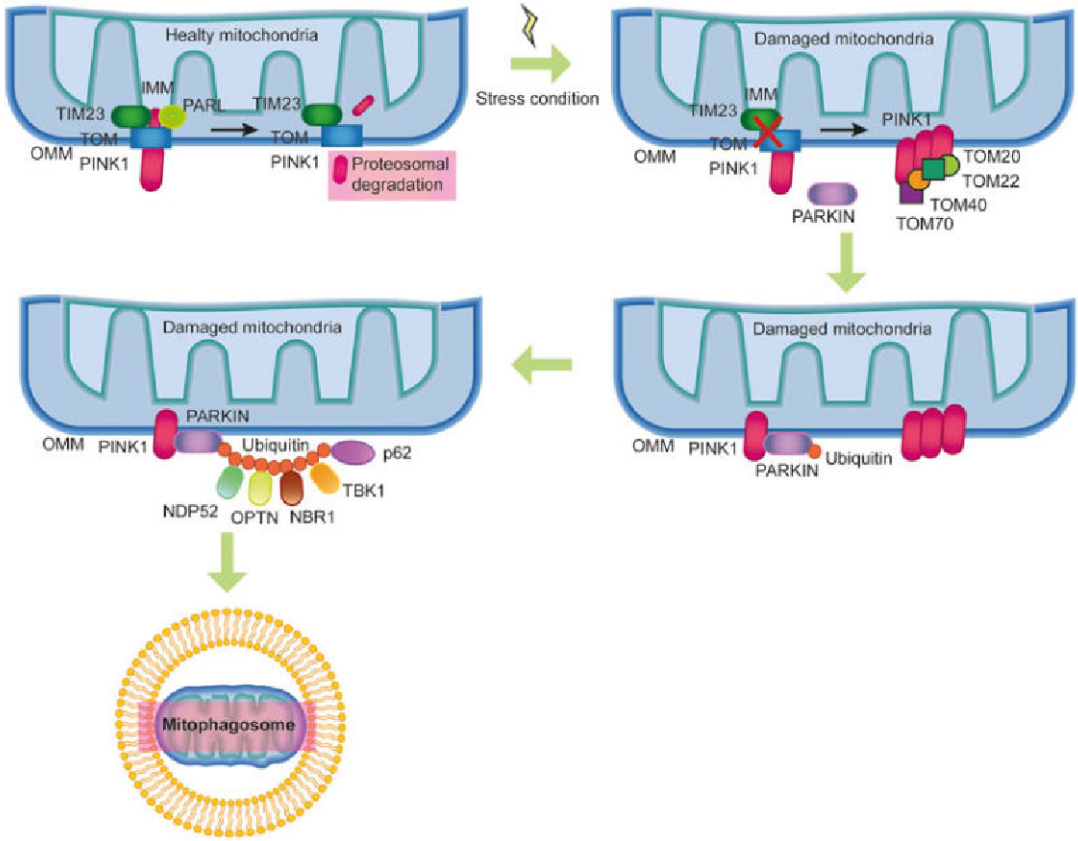

Fig. 1 Schematic representation of the molecular process of mitophagy. During resting conditions, PINK1 is imported into IMM via TIM-23-TOM activity. Here, PINK is cleaved by PARL in fragments, which are then degraded by proteasome. Upon damage, import of PINK1 is blocked leading to accumulation and stabilization in OMM surface, thanks to TOM proteins. In this conformation, PINK1 mediates phosphorylation events aimed to activate and recruit Parkin at OMM. Once activated, Parkin can elongate Ub chains, and a series of autophagic receptors (NDP52, OPTN, NBR1, TBK1, and p62) are recruited. Now, the damaged mitochondria can be surrounded by autophagosomal membrane to form the mitophagosome

[19, 20], PINK1 phosphorylates itself at S402, S228, and T257 and converts the autoinhibited E3-ubiquitin (Ub) ligase Parkin into an active phospho-Ub-dependent enzyme [21, 22]. In this active state, Parkin actively ubiquitinates several mitochondrial proteins at the OMM. Ubiquitination events promote the recruitment of the Ub-binding autophagy receptors p62/Sequestome, NBR1, NDP52, optineurin (OPTN), and TAX1BP1 (TBK1), which connect the damaged mitochondria to phagosomes for clearance in the lysosome (Fig. 1) [23–25].

1.1 Role of Mitophagy in Pathology

Mitochondria dysfunction and mitophagy defects are broadly implicated in numerous human diseases, including cardiovascular diseases (CVD), cancers, and neurodegenerative diseases. Below, we discuss contributions of mitophagy in pathologies, which are widely emergent in recent years.

1.1.1 Mitophagy in CVD

Mitophagy is essential for cardiovascular homeostasis and for cardiac mitochondrial quality control, as well as for the maintenance of the cardiac heart under both normal and pathophysiological conditions [26–29].

Aberrant mitophagy contributes to activate matrix metallopeptidase -9 (MMP-9), causing degradation of the important gap junction protein connexin-43 (Cx-43) in the ventricular myocardium. Reduction in Cx-43 levels was associated with increased fibrosis and ventricular dysfunction in heart failure. Recent insight by Tong M. and colleagues has shown that the suppression of mitophagy increased the accumulation of lipids in the heart during high-fat diet consumption. The same study revealed that the transcriptional activator (TAT)-Beclin1, which enhances mitophagy, tends to inhibit the development of diabetic cardiomyopathy [27].

Notably, PINK1 and Parkin protein levels are significantly decreased in type 1 diabetic hearts, resulting in decreased cardiac autophagy, which was correlated with reduced expression of the small GTPase Rab9, responsible for mitochondrial degradation during erythrocyte maturation in the absence of ATG5. Increased level of Rab9 protein was higher in mitochondria deficiency, suggesting that Rab9 mediated degradation of mitochondria in diabetic heart and contributed to mitophagy under certain conditions [30–32].

In recent investigated work, it has been found that sirtuin 1 (SIRT1), a deacetylase stimulated in response to several cardiac stresses to promote cell survival, promoted the induction of mitophagy in response to ER stress and eventually protected the cardiac cells from cell death. However, the inhibition of SIRT1 decreased ER stress-induced mitophagy. The whole-body deletion of PGAM family member 5 (PGAM5), a mitochondrial serine/threonine protein phosphatase, activates PINK1-mediated mitophagy in the heart. Moreover, PGAM 5 increased infarct size in mice with cardiac ischemia/reperfusion, which is implicated in mitophagy inhibition in the myocardium [33]. Hoshino and associates found that nuclear p53 attenuates mitophagy in the ischemic heart, which causes accumulation of altered mitochondria and increased myocardial damage [34]. The mitochondrial fission dynamin-1-like protein (DRP1), which is a critical fission regulatory, has an important role in the heart mitophagy. DRP1 deletion provokes mitophagic inhibition and consequent cardiac damage and enhanced risk to myocardial ischemia-reperfusion injury [35, 36].

Furthermore, DRP1 mutation C452F causes spontaneous development of monogenic-dilated cardiomyopathy with abnormal mitochondrial morphology and defective mitophagy [37].

Contrasting researches have revealed that mice lacking mitochondrial fusion or fission proteins manifest deteriorations in the developmental cardiac and increased susceptibility to cardiac injury [38, 39]. The ratio of mitofusin 2 (MFN2; a fusion protein) and

DRP1 (a fission protein) was decreased during heart failure, suggesting increased mitophagy [40]. Nevertheless, loss of the mitochondrial division DRP1and Parkin activates the mitophagic aberration and subsequently reduces mitochondrial respiration and provokes lethal cardiac aberrations.

1.1.2 Mitophagy in Cancer

Mitophagy prevents oncogenic transformation and maintains cellular homeostasis and eventually can be considered as a tumor suppressor process because selectively degrading impaired mitochondria can prevent the accumulation of ROS [1, 41]. The repression of mitophagy leads to an accumulation of impaired mitochondria and subsequently enhances tumorigenesis.

Increased evidence suggested the functional loss of mitophagy regulators in the development and the progression of cancer, and this became evident through the modulation of expression of the regulators including Parkin, BNIP3, NIX, and representative of tumor suppressor such as Rb, p53, and oncogenes like NF-kB, Hif-1a, and FOXO3 [42].

Interestingly, Parkin is a most frequently deleted gene in cancers; its deletion is associated with various types of cancer including serous ovarian breast carcinomas, liver, and colon cancer [43]. Besides its role in mitophagy, Parkin can behave as a tumor suppressor modulating the levels of various key cell cycle proteins, such as Cyclin D1, Cyclin E, and CDK4, all having a role in controlling G1/S progression. Further studies supported the notion that Parkin acts as a tumor suppressor: they knocked down Parkin and thus showed an increase in spontaneous liver tumors and sensitized mice to γ-irradiation-induced tumorigenesis [44].

Several insights showed that the dysregulation of proteins involved in the mitophagic process such as the promitophagic receptor BNIP3 has a tumor promoter role in melanoma, renal cell carcinoma, and pancreatic cancer, whereas in breast cancer, tumor suppressor functions [45]. Furthermore, knocking down BNIP3 stimulates tumor formation and metastasis in mouse model, suggesting a key role of mitophagy in suppressing cancer development [42]. Again, BNIP3 is frequently been deleted in triple-negative breast cancer (TNBC) and epigenetically silenced in other types of cancer including gastric, lung, liver, and pancreatic cancer [42]. Hypoxia occurs in solid tumor. It has been found that HIF-1α plays a crucial role in adaptation of cancer cells under hypoxic condition, and it enhances the expression of BNIP3. Furthermore, an enhanced expression of HIF-1α has been found in hemangioblastoma, glioblastoma multiforme, breast and prostate cancer, colonic adenocarcinoma, and subtypes of the lung [46].

1.1.3 Mitophagy in Neurodegenerative Diseases

Mitophagy plays a protective role in numerous neurodegenerative diseases via mitophagy by clearing impaired mitochondria in neuronal axon, and genetic aberrations in both PINK and Parkin have been associated with the development of hereditary PD [47].

Mutations in α-synuclein (α-syn), a component of Lewy bodies, the pathological hallmark of PD, leads to a block in mitophagy [48]. Overexpression of A53T α-syn mutant leads to a stimulation of p38 MAPK and thus phosphorylated Parkin at SER131 to disrupt its functions [49]. Recently, the activity of α-syn has been correlated to the activity of mitochondrial Rho GTPase 1 (Miro1). This protein anchors mitochondria to microtubule motors and is required for mitochondrial motility in healthy conditions to stop mitochondrial motility and initiate mitophagy, Miro1 should be removed. On the contrary, α-syn interacts with Miro1 via its N-terminus and enhances Miro1 protein levels, thus leading to an abnormal Miro1 accumulation on the mitochondrial surface and delayed mitophagy [50].

Other genes and proteins that can mediate between mitochondrial autophagy and the progression of PD. The protein DJ1, associated with a rare form of autosomal recessive PD, is localized to mitochondria, where it regulates the removal of endogenous ROS and the mitophagy process [51, 52]. Deletion of DJ1 enhanced the recruitment of Parkin to damaged mitochondria and increased mitochondrial autophagy [53].

Leucine-rich repeat kinase 2 (LRRK2) is present in the mitochondria, modulates mitochondrial homeostasis, and represents the major risk factor for PD and it having been shown to be correlated with sporadic and hereditary PD. G2019S, one of the most frequent LRRK2 mutations implicated in PD, leads to fission of mitochondria via an increased DRP1 activity, followed by activation of mitophagy [54].

In addition, dysfunctional mitochondria are found in diseases of the peripheral nerves, including the inherited axonal neuropathies, Charcot-Marie-Tooth neuropathy disease type 2 (CMT2A) is commonly associated with aberrations in proteins linked to mitochondrial dynamic including MFN2 and GDAP1 [55]. A recent work showed that motor neuron of CMT2A patients and expressing mutant MFN2 exhibit defects in mitophagy. These findings highlight the importance of mitophagy process to axonal homeostasis [56].

Parkin is also associated with the progression of Alzheimer's disease (AD) [57]. Human wild-type full-length Tau (hTau) affects the mitochondrial membrane, thereby causes mitochondrial dysfunction. A recent evidence found that both hTau and familial forms of frontotemporal dementia (FTD) mutant Tau (hP301L) suppressed mitophagy in neuroblastoma cells via the reduction of Parkin. The hTau NH_2-terminal fragment modulates Parkin via the repression of ANT-1-dependent ADP/ATP exchange, inhibits mitophagy, and affects synaptic degeneration in AD [58].

Sirtuins family are NAD^+-dependent enzymes disrupted in AD and contributing to AD pathogenesis. Increased evidence reported that SIRT1 modulates multiple pathways that go amiss in AD, including neuroinflammation, neurodegeneration, and mitochondrial alterations [59]. Resveratrol has been shown to enhance the expression of SIRT1 and can upregulate the level of LC3-II/LC3-I, Beclin 1, and Parkin, reduce the positioning of LC3 and TOM20, as well as regulate BNIP3- and NIX-related pathways in AD-excessive SIRT2 stimulation leading to mitochondrial alteration and ensuing mitophagy [60].

Alteration in mitophagy is linked also to Huntington's disease (HD). Dysfunctional mitochondria are correlated with different animal models of HD, and mutant huntingtin (mhtt) influences mitochondrial biogenesis and function and affects negatively the mitochondrial delivery to the lysosome [61]. In addition, valosin-containing protein (VCP), known as p97, is located in various subcellular organelles, such as ER, nucleus, and mitochondria, where it has different functions including regulation of ER and mitochondria degradation, autophagy, and DNA repair [62]. An elegant work has shown that VCP selectively translocates to the mitochondria and acts as an mtHtt-binding protein on the mitochondria. Accumulated in mitochondria, VCP elicits excessive activation of mitophagy, inducing neuronal cell death. By adding the HV-3 peptide, VCP translocation to the mitochondria is abolished, the excessive mitophagy is inhibited, determining a reduction of cell death in both HD mouse/patient-derived cells and HD transgenic mouse brains [63].

The α-tubulin deacetylase HDAC6 is a cytosolic histone deacetylase suggested to block mitophagy. Thus, inhibiting HDAC6 increases neuronal vesicular flux and is considered as a potential therapeutic to treat HD, but the mechanisms remain unclear [64, 65]. Several evidence in cell lines suggest the role of HDAC6 for autophagosome–lysosome fusion and also that HDAC6 promotes the removal of mHtt and impaired mitochondria [66, 67].

In amyotrophic lateral sclerosis (ALS), mitochondria are damaged and accompanied with the depletion of motor neuron disease (MND) and upper motor neuron (UMN). Increased evidence suggest the potential role of mitophagy in ALS. More than 30 gene mutations including OPTN, TBK1, VCP, C9ORF72, and SOD1 are linked to ALS. Consistently, loss of function mutations in genes TBK1 and OPTN are involved in the impairment of mitophagy pathway and accumulation of damaged mitochondria [68].

Approximately, 20% of the ALS are caused by aberration of SOD1, which was the first ALS gene discovered [69]. For instance, mutant SOD1 causes mitochondrial dysfunction and contributes to motor neuron demise in ALS, thus stimulating mitochondria

quality control (MQC) to reduce impaired mitochondria accumulation via mitophagy process [70, 71]. It has been reported that SOD1 relies on PINK1 to decrease the mitochondrial dynamic protein Miro1. Mutant SOD1 altered axonal transport in PINK1/Parkin pathway-dependent manner [72].

2 Monitoring Mitophagy Using Fluorescent Probes

To determine the colocalization of mitochondria with either autophagosomes or lysosomes, represent the main method to measure mitophagy [73]. The colocalization of mitochondria with autophagosome can be studied by using a green fluorescent protein (GFP)-LC3 plasmid (for autophagosome labeling) and a mitochondrially targeted red fluorescent protein (RFP) (to visualize mitochondria) [74]. Alternatively, it is possible to monitor the delivery of sequestered mitochondria to the lysosome by using the fluorescent dyes MitoTracker and LysoTracker [75] or the mitochondrial pH-dependent Keima protein (named mito-Keima). This fluorescent protein changes color depending on the pH environment, and when mitochondria undergoing mitophagy are sequestered into the lysosomal compartment, the peak of excitation of mito-Keima shifts from green (neutral pH) to red (acidic) color [76, 77].

Following a PINK1 stabilization, Parkin protein translocates from cytosol to mitochondria. Fluorescent recombinant chimeras of Parkin, such as mCherry-Parkin, permit to monitor this translocation and thus understand when the mitophagic process is activated at OMM surface. The same information may be obtained performing an immunofluorescence assay against Parkin and a mitochondrial marker [78, 79]. In the following sections, we will describe two different assays for monitoring and quantifying the mitophagic levels by using a fluorescence approach.

2.1 Colocalization Autophagosome and Mitochondria by Confocal Fluorescent Microscopy

2.1.1 Materials

1. Biological material (cell cultures of interest) (*see* **Note 1**).
2. Culture medium Dulbecco's Modified Eagle Medium (DMEM; e.g., Gibco 11965084) supplemented with 10% fetal bovine serum (FBS), 1% penicillin-streptomycin, and 1% L-glutamine.
3. Glass coverslips 24 mm in diameter (*see* **Note 2**).
4. Six-well culture plates.
5. 1× phosphate-buffered saline (PBS) buffer, pH 7.4, no phenol red. In 1 l of distilled water, add 8 g of NaCl, 0.2 g of KCl, 1.44 g of Na_2HPO_4, 0.24 g of KH_2PO_4. Adjust the pH to 7.4 with HCl.
6. 10 mM carbonyl cyanide 4-(trifluoromethoxy)phenylhydrazone (FCCP).

7. Plasmid encoding for a fluorescent mitochondrial probe, that is, mCherry-mito7 [80] mt-DsRed [81] (*see* **Note 3**).
8. DNA transfection reagent, that is, jetPEI® (PolyPlus transfection, 101-10 N).
9. Attofluor cell chamber (e.g., ThermoFisher, A7816).
10. 4% paraformaldehyde (PFA) solution, pH 7.4, in 1× PBS. Add 4 g of PFA in 100 ml of 1× PBS.
11. Inverted Zeiss LSM 510 confocal microscope.

2.1.2 Methods

1. Plate cells onto coverslips (24 mm in diameter) at a density of 100,000 cells per well in a 6-well plate.
2. Let the cells grow on the cover slip surface to achieve 60–75% confluence.
3. Transfect cells with 1 μg/coverslips GFP-LC3 plasmid and mCherry-mito7 by using the appropriate method.
4. After 4–6 h, replace the transfection medium with warm medium culture.
5. Wait for 24–48 h (*see* **Note 4**).
6. Add a final concentration 1 μM of FCCP to provoke mitophagy (*see* **Note 5**).
7. After 3 h, image the cells. Alternatively, cells can be fixed in 4% PFA 15 min at room temperature (RT), washed three times with 1× PBS, and stored at 4 °C in the dark (*see* **Note 6**).
8. Move the coverslips into a cell chamber and place in a 37 °C thermo-controlled stage of the inverted Zeiss LSM 510 confocal microscope (*see* **Note 7**). Fluorescence images are captured providing excitation at 488 nm (green) and 546 nm (red) with detection of green (500–540 nm) and red (580–640 nm) fluorescence signals.
9. To obtain a statistical measurement, acquire at least 20–25 images per condition (*see* **Note 8**).

2.1.3 Data Handling

Image processing may be achieved by using the microscope software (ZEN elements for Zeiss instruments) or Fiji software. After background subtraction on both green and red channels, generate merged images to visualize the colocalization amounts (Fig. 2). To quantify the yellow signal, we suggest using the colocalization plug-in available in Fiji software or the colocalization command of ZEN element software. Alternatively, it is possible to perform a simple count of yellow dots or measure the intensity profile of a region of interest (ROI) for both red and green channels (*see* **Note 9**).

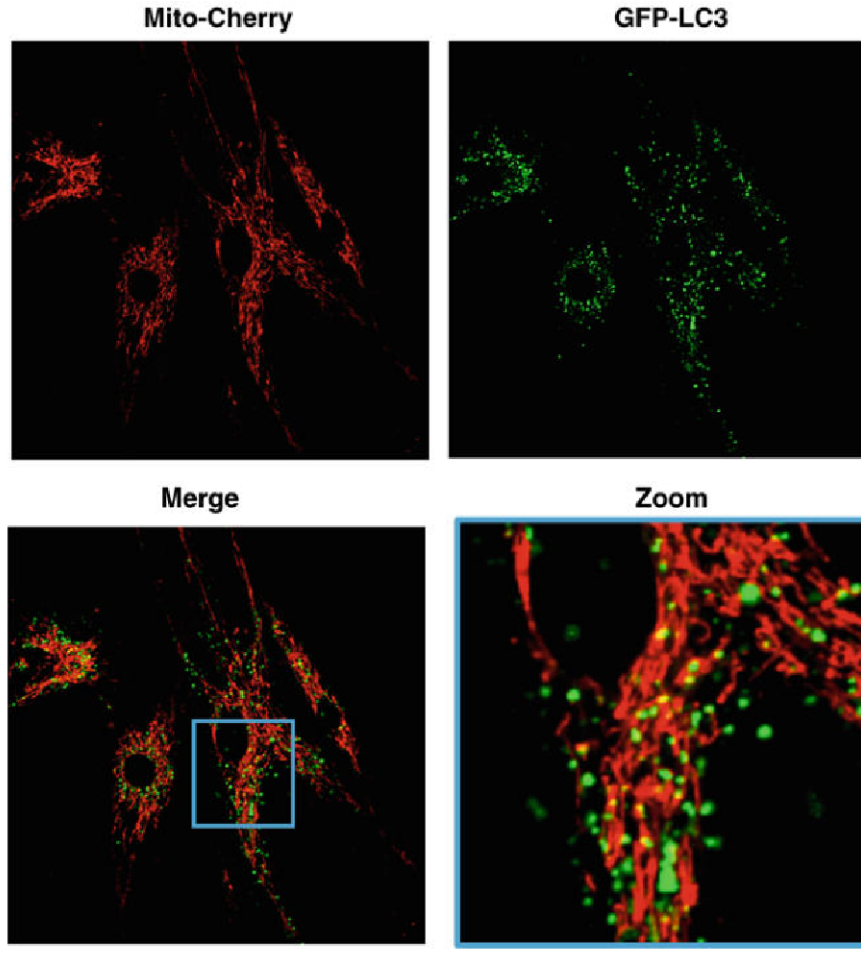

Fig. 2 Colocalization of the autophagosomal marker GFP-LC3 and mitochondria. After transfection, cells were treated with FCCP to cause mitochondrial damage and the accumulation of autophagosome. LC3 (green) and mitochondrial (red) signals were then recorded by using a fluorescence confocal microscope equipped using an oil 63× 1.4 NA lens, and the colocalization rate was investigated by merging the channels. The regions indicated in blue box are enlarged in the Zoom panel. Yellow dots are representative of colocalization of GFP-LC3 and mCherry-mito7. Scale bar 10 μm

2.1.4 Notes

1. It is also possible to use cells with stable expression of GFP-LC3 construct. However, the establishment of a stable cell line requires a significant investment of time. In addition to this, stable cell lines are often immortalized tumor cell lines and are far from the physiology of primary cells.
2. Alternative supports are cell imaging dishes 35 mm in diameter.
3. To stain mitochondrial structures, a large series of mitochondrial-specific fluorescent dyes (MitoTracker Green, MitoTracker Orange, MitoTracker Red, and MitoTracker Deep Red) may be used.

4. Certain transfection protocols may induce autophagy. We recommend leaving the cells for a period of 48 h posttransfection to allow equilibration [82].
5. Adjust the FCCP concentration according to the cell type used.
6. Fixation procedure may produce autofluorescent puncta or a reduction of GFP-LC3 staining.
7. Changes in temperature and prolonged light exposure during live-cell imaging may provoke photodamage and photobleaching. Keep laser potency and exposure time low.
8. Keep exposure time and illumination constant across samples.
9. The overlay of the channels of interest possesses some limitations. The merged staining may be dependent on the signal intensity of each channel. To avoid artifacts, we suggest verifying the result obtained by using algorithms performing intensity correlation coefficient-based analyses (ICCB), such as Pearson's or Manders' coefficients and object-based approaches (such as the centroid or intensity center calculation).

2.2 Colocalization Parkin and Mitochondrial Marker

2.2.1 Materials

1. Biological material (cell cultures of interest).
2. Culture medium Dulbecco's Modified Eagle Medium (DMEM; e.g., Gibco 11965084) supplemented with 10% FBS, 1% penicillin-streptomycin, and 1% L-glutamine.
3. Glass coverslips 24 mm in diameter (*see* **Note 1**).
4. Six-well culture plates.
5. 1× PBS buffer, pH 7.4, no phenol red. In 1 l of distilled water, add 8 g of NaCl, 0.2 g of KCl, 1.44 g of Na_2HPO_4, 0.24 g of KH_2PO_4. Adjust the pH to 7.4 with HCl.
6. Permeabilization Buffer: 0.05–0.3% Triton X-100 (or 100 μM digitonin or 0.5% saponin) in 1× PBS.
7. Blocking Buffer (chose one of below):
   - 5–10% serum from host species of secondary antibody (blocking).
   - 1–3% bovine serum albumin (BSA) in 1× PBS.
8. 4% PFA solution, pH 7.4, in 1× PBS. Add 4 g of PFA in 100 ml of 1× PBS.
9. Primary antibody mouse anti-ATP5A (abcam, ab14748) (or another mitochondrial marker).
10. Primary antibody rabbit anti-Parkin (ThermoFisher, PA5–13398).
11. Secondary antibody Alexa Fluor 488 goat anti-rabbit (ThermoFisher, A27034).

12. Secondary antibody Alexa Fluor 647 goat anti-mouse (ThermoFisher, A28181).
13. Antigen Retrieval Buffer (ARB): 100 mM Tris, 5% (w/v) urea, pH 9.5.
14. Inverted Nikon confocal microscope system A1 R (*see* **Note 1**).

2.2.2 Methods

Sample Preparation and Transfection

1. Plate cells onto coverslips (24 mm in diameter) at a density of 100,000 cells in a 6-well plate.
2. Wait at least for 24 h.
3. After three washes with 1× PBS, fix cells in 4% PFA 15 min at RT.
4. Wash three times with 1× PBS (*see* **Notes 2** and **3**).
5. Add 1 ml of permeabilization buffer in each well. Incubate for 10 min at RT with agitation.
6. Wash three times with 1× PBS.
7. Incubate cells with 1 ml of blocking buffer for 30 min at RT with agitation to block unspecific binding of the antibodies (*see* **Note 4**).
8. Incubate cells in the diluted antibody in 1% BSA in 1× PBS in a humidified chamber for 1 h at RT overnight (ON) at 4 °C (*see* **Note 4**).
9. Wash three times with 1× PBS.
10. Incubate cells with the secondary antibodies in 1% BSA in 1× PBS for 1 h at RT in the dark. We recommend a dilution range of 1:500–1:1000.
11. Wash three times with 1× PBS.
12. Mount coverslips with a drop of mounting medium (*see* **Note 5**).
13. Store in the dark at 4 °C or − 20 °C.

Measurement

14. Move the coverslips in a controlled stage of the inverted microscope (*see* **Note 3**). Fluorescence images are captured, providing excitation at 488 nm (green) and 647 nm (deep red) with detection of green (500–540 nm) and red (650–720 nm) fluorescence signals (*see* **Note 4**).
15. To obtain a statistical measurement of the mitochondrial network, acquire at least 20–25 images per condition (*see* **Note 5**).

2.2.3 Data Handling

Image processing may be achieved by using the microscope software (NIS elements for Nikon instruments) or Fiji software. After background subtraction on both green and red channels, generate merged images to visualize the colocalization amounts. To quantify the yellow signal, we suggest using the colocalization plug-in available in Fiji software or the colocalization command of NIS-element software (Fig. 3). Alternatively, it is possible to perform a simple count of yellow dots or measure the intensity profile of a ROI for both red and green channels.

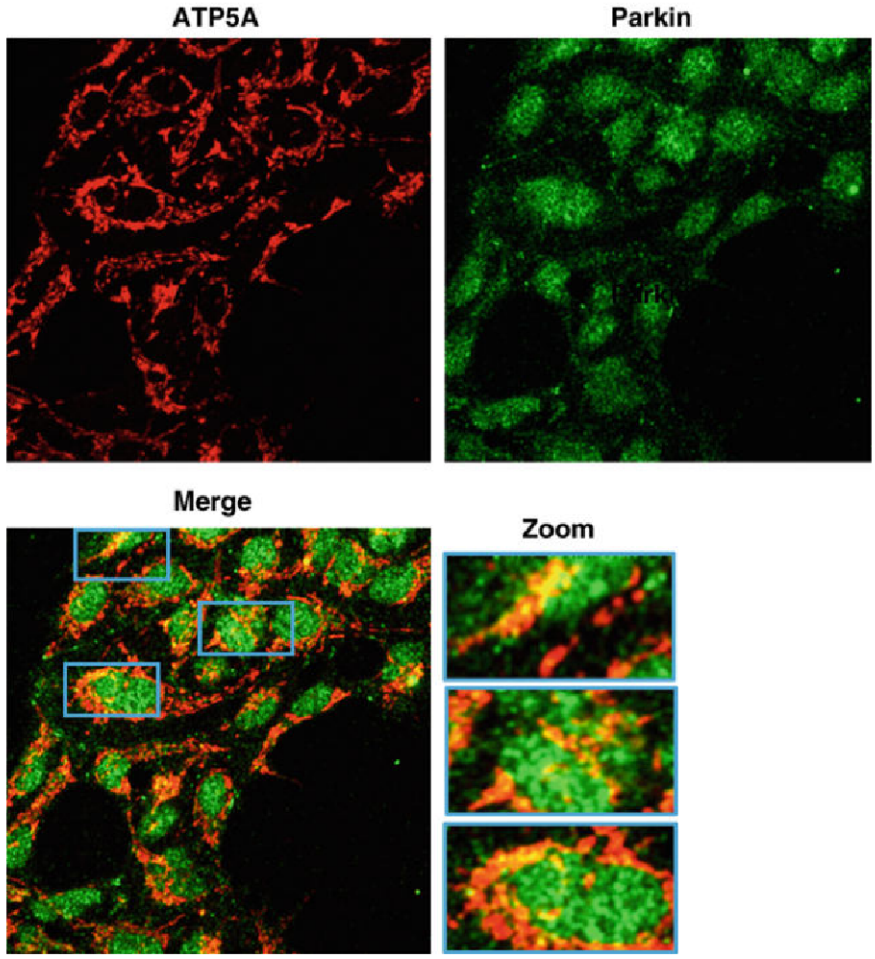

Fig. 3 Colocalization Parkin and mitochondrial marker. Cells were fixed, permeabilized, and exposed to primary antibodies against ATP5A (mitochondrial marker, red) and Parkin (green). After incubation with secondary antibodies, cells were imaged in a confocal inverted microscope, and the colocalization rate was investigated. Regions in blue box are enlarged in the Zoom panels. Yellow dots are representative of colocalization of Parkin and mitochondria. Scale bar 10 μm

2.2.4 Notes

1. Alternative supports are glass coverslips 13 mm in diameter or cell imaging dishes 35 mm in diameter.
2. Before permeabilization, it is possible to perform the antigen retrieval by preheating the coverslips with the ARB at 95 °C. After 10 min, remove the coverslips and wash cells in PBS three times for 5 min.
3. Proceed with permeabilization or keep sample immerged in PBS at 4 °C for 1 week.
4. Blocking and primary antibody buffers may be supplemented with 0.01% Triton X-100 (or 10 μM digitonin or 0.1% saponin).
5. We recommend sealing coverslips with nail polish to prevent drying.

3 Monitoring Mitophagy Using Nonfluorescence Methods

Undoubtedly, fluorescence methods are the most used techniques to study mitophagy. However, these assays only demonstrate colocalization of the autophagosome with mitochondria. They cannot be used to determine mitochondrial degradation. Furthermore, the use of fluorescent indicators may have several limitations. For example, MitoTracker dyes are dependents of mitochondrial potential. Changes in lysosomal pH can affect the staining pattern of Lyso tracker. GFP-LC3 puncta are not always autophagosomes and may form aggregates that give misleading results. Clearly, other approaches measuring mitophagy should be combined with these assays to confirm the results obtained.

Transmission electron microscopy (TEM) is one of the most powerful approaches for the evaluation of mitophagy. Fulfilling the philosophy of "seeing is believing," the principle of this analysis is the direct identification of autophagosomes and autophagolysosomes that have physically engulfed a mitochondrial particle, by visual inspection. Indeed, the high resolutive power of TEM allows recognition of the morphological features, which characterize autophagosomes, autophagolysosomes, and mitochondria. It should be noted that mitophagy evaluation by TEM could sometimes be problematic. This is mainly due to: (1) poor sampling of the phenomenon (depending on the cell orientation, during cutting autophagosomes might appear in the section or not), (2) methodological artifacts deriving from fixation, which might lead to misinterpretation, and (3) a specialized training to operate at is required.

Considering these remarks, complementary techniques should be considered. Following, we will describe two methods determining the mitochondrial autophagy by using immunoblot and enzyme-linked immunosorbent assay (ELISA) procedures.

3.1 Evaluation of Mitochondrial Protein Amounts

The final step of mitophagy is the removal of the sequestered mitochondria [24].

Western blotting can be used to measure mitochondrial protein degradation to determine whether mitophagic process is activated. When this experiment is conducted, all mitochondrial compartment proteins (including matrix proteins) should be analyzed. The only detection of outer mitochondrial membrane proteins, described to be mitophagic targets (TOM20, VDACs, and mitofusins), can mislead the result because these proteins are also degraded by the proteasome.

3.1.1 Materials

1. Biological material (cell cultures of interest).
2. Culture medium Dulbecco's Modified Eagle Medium (DMEM; e.g., Gibco 11965084) supplemented with 10% FBS, 1% penicillin-streptomycin, and 1% L-glutamine.
3. FCCP (*see* **Note 1**).
4. Radioimmunoprecipitation (RIPA) lysis buffer (150 mM sodium chloride, 1.0% NP-40 or Triton X-100, 0.5% sodium deoxycholate, 0.1% sodium dodecyl sulfate (SDS), 50 mM Tris, pH 8.0, supplemented of protease and phosphatase inhibitors).
5. Transfer Buffer 1× (1 l): Tris base 5.8 g, glycine 2.9 g, SDS 0.37 g. Make 800 ml with dH_2O, then add 200 ml MeOH.
6. Tris-Buffered Saline (TBS; 10×): 1.5 M NaCl, 0.1 M Tris–HCl, pH 7.4.
7. TBS containing 0.05% Tween-20 (TBS-T).
8. Blocking Solution: 5% milk in TBS-T.
9. Precast gel 4–12% Bis-Tris Bolt (ThermoFisher, NW04120BOX).
10. Nitrocellulose or PVDF membranes.
11. Primary antibody anti-HSP60 (mitochondrial matrix marker, mouse, Santa Cruz, sc-13115), anti-TIM23 (inner mitochondrial membrane marker, mouse, BD Bioscience, 611222), and anti-pan/VDAC1 (outer mitochondrial membrane marker, rabbit, abcam, ab34726) (*see* **Note 2**).
12. Primary antibody anti-GAPDH (loading marker, rabbit cell signaling, 5174).
13. Primary antibody anti-PDI (ER marker, rabbit, cell signaling, 2446) (*see* **Note 3**).
14. Restore western blot stripping buffer (ThermoFisher, 21059).

3.1.2 Method

Sample Preparation and Homogenates Collection

1. Plate cells in 6-well plates at a density of 150,000 cells.
2. After at least 24 h, treat cells with a strong mitophagic inducer, such as 100 nM FCCP.

3. Collect cellular homogenates and lyse them with RIPA lysis buffer. Keep homogenates in ice. After 30 min, centrifuge cell lysates at 12,000 × *g* for 10 min at 4 °C, collect the supernatant, and keep them at −80 °C.

Western Blot.

After having determined the protein concentration for the cell lysate, prepare the sample (10–15 μg of proteins) in denaturating conditions and boil the mixture at 95–100 °C for 5 min.

4. Load samples in a precast gel 4–12% and perform the electrophoresis at 150 mV for 30–45 min.
5. Following electrophoresis, activate PVDF with methanol for 1 min and rinse with transfer buffer. If a nitrocellulose membrane is used, only rinse it with transfer buffer. Assemble the transfer stack with sponges, filter papers, membrane, and gel, being careful to that the gel is facing the cathode (−) and the membrane side is facing the anode (+). We recommend transferring the gel for 2 h at 350 mA.
6. After the protein transfer, rinse the membrane in TBS-T and place the membrane in blocking solution and incubate with agitation for 1 h.
7. Place the blot in the primary antibodies solution and incubate with agitation overnight. Wash the blot three times for 5 min.
8. Place the blot in the secondary antibody solution and incubate with agitation for 1 h at RT. Wash the blot three times for 5 min.
9. Proceed with chemiluminescent detection.

In the case some proteins have similar molecular weight, stripping and reprobing the blot as follows:

10. After detection, wash blot to remove chemiluminescent substrate.
11. Incubate blot in Restore western blot stripping buffer for 15 min at RT. Wash the blot three times in TBS-T with agitation for 10 min at RT.
12. Place the membrane in blocking solution and incubate with agitation for 1 h.
13. Place the blot in the primary antibodies solution and incubate with agitation O.N. Wash the blot three times for 5 min.
14. Place the blot in the secondary antibody solution and incubate with agitation for 1 h at RT. Wash the blot three times in TBS-T with agitation for 10 min at RT.
15. Proceed with chemiluminescent detection.

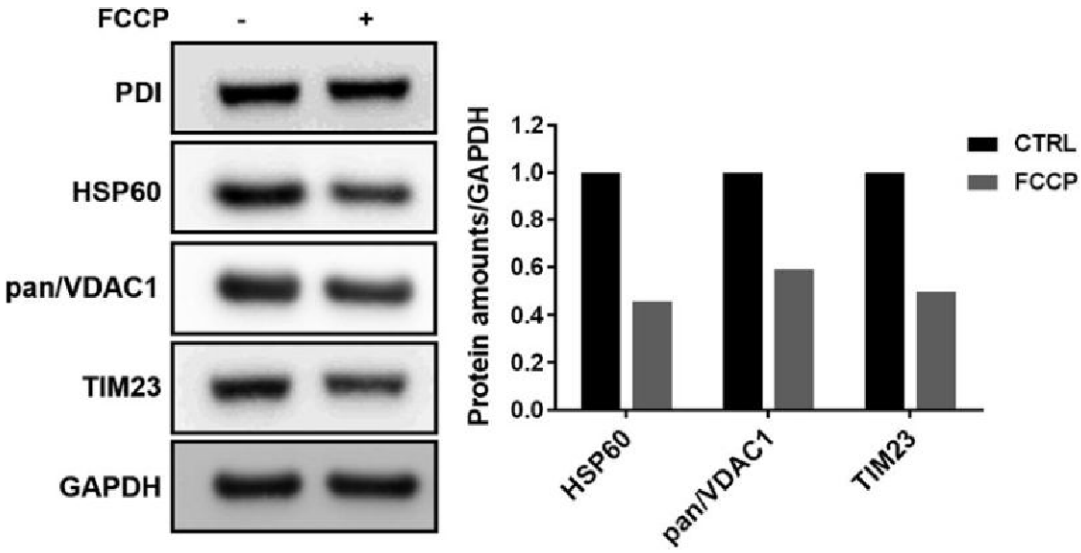

Fig. 4 Evaluation of mitochondrial protein amounts. Levels of mitochondrial proteins were analyzed by western blot. Primary antibodies against HSP60 (matrix marker), pan/VDAC1 (OMM marker), and TIM23 (IMM marker) were used, and the specific levels measured were normalized with GAPDH. PDI (ER marker) was used as control

3.1.3 Data Handling/ Processing

Quantify the bands with a densitometric program and then divide the protein amounts of each mitochondrial marker with the loading marker.

3.1.4 Notes

1. To detect mitochondrial protein degradation is necessary to have high levels of mitophagy. We suggest using this technique following treatment with a mitochondrial stressor inducer like FCCP.
2. Considering that is not clear whether mitophagy is the only cellular mechanism to remove mitochondria, it is recommended to verify the protein amounts of all mitochondrial subcompartments.
3. To ensure that the protein loss is limited to the mitochondrial compartment, it is recommended to verify the protein amounts of another intracellular compartment (e.g., ER proteins) (Fig. 4).

3.2 Parkin Translocation by Subcellular Fractionation

Mitophagy is a homeostatic process that targets unwanted and altered mitochondria to autophagosomes with subsequent degradation in autolysosomes. The selectivity of mitophagic response is achieved through specific mitophagic receptors (such as NDP52 and OPTN), which recognize cargos tagged with degradation signals as well as the autophagosomal membrane protein LC3 [25, 83, 84]. NDP52 and OPTN are cytosolic receptors recruited by PINK1 in the first steps of mitophagy. They are responsible to

recognize the damaged mitochondria and to promote its sequestration into phagosome. To potentiate the mitophagic response, PINK1 phosphorylates Parkin, an E3 ubiquitin ligase that translocates to altered mitochondria to increase the rate of phagosome formation. Parkin recruitment to mitochondria leads to ubiquitination of several targets including mitochondrial fusion proteins, such as mitofusins [85, 86], which promotes mitochondrial fragmentation prior to engulfment by the phagosome [87].

Evaluate the accumulation of mitophagic markers to alter mitochondria is an easy and well-established approach to study the activation of mitophagic response in the cells. With the subcellular fractionation protocol, here described, it is possible to obtain highly purified mitochondria fraction from cultured cells and liver, where analyze the expression levels of mitophagic markers accumulated.

3.2.1 Materials

1. Biological Material: cell lines of interest or liver biopsy.
2. 1× PBS buffer, pH 7.4, no phenol red. In 1 l of distilled water, add 8 g of NaCl, 0.2 g of KCl, 1.44 g of Na_2HPO_4, 0.24 g of KH_2PO_4. Adjust the pH to 7.4 with HCl.
3. FBS (ThermoFisher, 10270106).
4. Phosphatase inhibitor cocktail (100×) (Merck, P0044).
5. Protease inhibitor cocktail (100×) (Merck,P8340).
6. 1 l of Tris–HCl 1 M (pH 7.4): Dissolve 121.14 g of Trizma-Base in 500 ml of bidistilled water, adjust pH to 7.4 using HCl, bring the solution to 1 l with bidistilled water and store at 4 °C.
7. ½ l of 4-(2-hydroxyethyl)-1-piperazineethanesulfonic acid (HEPES) 0.5 M (pH 7.4): Dissolve 59.57 g of HEPES in 400 ml of bidistilled water, adjust pH to 7.4 using KOH, bring the solution to 500 ml with bidistilled water and store at 4 °C.
8. 100 ml of 100 mM Ethylene-bis(oxyethylenenitrilo)tetraacetic acid (EGTA) (pH 7.4): Dissolve 3.8 g of EGTA in 70 ml of bidistilled water, adjust pH to 7.4 with KOH, bring the solution to 100 ml with bidistilled water and store at 4 °C.
9. ½ l of Homogenization Buffer (HB) for Cells: (Composition: mannitol 225 mM, sucrose 75 mM, and 30 mM Tris–HCl, pH 7.4). Dissolve 20.5 g of mannitol, 13 g of sucrose in 400 ml of bidistilled water and add 15 ml of 1 M Tris–HCl (pH 7.4). Leave the buffer for about 30 min at 4 °C to cool down. Check the pH of the buffer and adjust if necessary with KOH (if too low) or HCl (if too high) and bring the solution to a final volume of 500 ml with bidistilled water and store at 4 °C. The buffer needs to be prepared fresh and must be free of protease and phosphatase inhibitor cocktails to avoid sample alteration. For liver homogenization: (composition: 225 mM

mannitol, 75 mM sucrose, 0.5% BSA, 0.5 mM EGTA, and 30 mM Tris–HCl, pH 7.4). Dissolve in 150 ml of HB for cells 0.75 g of albumin and 0.75 ml of 100 mM EGTA (pH 7.4) and store at 4 °C.

10. 100 ml of Mitochondria Isolation Buffer: (Composition: 250 mM mannitol, 5 mM HEPES (pH 7.4), and 0.5 mM EGTA). To prepare 100 ml of mitochondria isolation buffer, dissolve 4.56 g of mannitol in 80 ml of bidistilled water, add 1 ml of 0.5 M HEPES (pH 7.4) and 0.5 ml of 100 mM EGTA (pH 7.4). Check the pH of the buffer and adjust if necessary and bring the solution to a final volume of 100 ml with bidistilled water and store at 4 °C. This buffer needs to be prepared fresh and must be free of protease and phosphatase inhibitor cocktails to avoid sample alteration (*see* **Notes 1–3**).
11. Cell culture dishes, 100 mm in diameter.
12. Cell scrapers (Sarstedt, 83.1830).
13. Stirrer motor with electronic speed controller (Cole-Palmer, EW-04369-10).
14. Motor-driven tightly fitting glass/Teflon Potter-Elvehjem homogenizer.
15. Loose- and tight-fitting glass Potter dounce homogenizer.
16. Oak Ridge Nalgene 30 ml tubes (for Sigma rotor angular 6 × 30 ml, Model 12139).
17. 1.5 ml Eppendorf microfuge test tubes (Eppendorf AG, 0030 120.086).
18. SW 40 rotor (swinging bucket, 6 × 14 ml, 40,000 rpm, 285,000 × *g*) (Beckman, 331302).
19. Sigma rotor angular 6 × 30 ml (Merck, 12139).
20. Refrigerated Sigma low-speed centrifuge (Sigma (Braun), Model 2 K15, tabletop).
21. Low-speed MPW 342 centrifuge with rotor no. 12108.

3.2.2 Method

Solutions, centrifuge, rotor, centrifuge tubes, and homogenizer should be prechilled to 4 °C. Carry out all procedures at 4 °C or working in ice.

For Adherent Cells:

1. Amplificate cells in petri dishes, to obtain at least two confluent petri for experimental conditions. In our experience, it is minimum number of plates useful to isolate a sufficient amount of mitochondria.
2. Discard the medium in culture dishes and wash the cells with ice-cold 1× PBS.

3. Scrape the adherent cells using cell scraper, then collect the cells in centrifuge tube.
4. Centrifuge the cells at 400 × *g* for 5 min at 4 °C. Remove the supernatant and resuspend the pellet in 1 ml of ice-cold homogenization buffer.
5. Transfer the cells to glass/Teflon-dounce Potter homogenizer.
6. Homogenize the cells using a tight pestle of dounce potter, every 25 strokes, and control cell integrity under a light microscope (*see* **Note 4**).
7. Finish homogenization when 80–90% of cell damage has been attained.

For Liver:

8. Rinse the murine liver twice with ice-cold 1× PBS.
9. Remove gallbladder and transfer the liver into a 50 ml tube. Wash the liver using ice-cold homogenization buffer for liver.
10. Discard the bloody homogenization buffer and repeat the wash for three times.
11. Using scissors, cut the liver in small pieces.
12. Collect the liver pieces and wash once again with ice-cold homogenization buffer for liver.
13. Discard the bloody homogenization buffer, transfer the liver pieces to the glass/Teflon Potter homogenizer. Add homogenization buffer for liver in the ratio 4 ml of buffer per gram of liver.
14. Homogenize the liver pieces using a pestle by eight strokes. Check the integrity of homogenized cells under a light microscope.

Once Obtained the Homogenized Cells:

15. Collect an aliquot (homogenate fraction) for western blot analysis. Add to homogenate aliquot the protease and phosphatase inhibitor cocktails then store at −20 °C.
16. Transfer the homogenized cells to 30 ml polypropylene centrifugation tubes, centrifuge at 600 × *g* for 5 min at 4 °C.
17. Transfer the supernatant to clean centrifuge tube and discard the pellet.
18. Repeat once again the centrifugation at 600 × *g* for 5 min at 4 °C.
19. Transfer the resulting supernatant to clean centrifuge tubes and discard the pellet.
20. Centrifuge the resulting supernatant at 15,000 × *g* for 10 min at 4 °C.

21. Collect the supernatant (cytosolic fraction containing lysosomes and microsomes contamination) in a clean centrifuge tube to prepare the cytosolic fraction, while the pellet will be resuspended in mitochondria isolation buffer (see below).

Preparation of the Cytosolic Fraction

22. Centrifuge the resulting supernatant at 17,000 × *g* for 30 min at 4 °C, to eliminate the lysosomes.
23. Collect the resulting supernatant in a clean tube, centrifuge at 100,000 × *g* for 90 min at 4 °C, to separate the cytosolic and ER fractions.
24. Collect the resulting supernatant (cytosolic fraction) and add the protease and phosphatase inhibitor cocktails for western blot analysis, then store at −20 °C.
25. The pellet (ER fraction) may be resuspended in homogenization buffer per western blot analysis.

Preparation of Mitochondrial Fraction

26. Gently wash the pellet with mitochondria isolation buffer without resuspending the pellet.
27. Gently discard the buffer, then resuspend the pellet by repeated pipetting in 1 ml of mitochondria isolation buffer.
28. Complete the resuspension of the mitochondrial pellet, using a loose pestle of dounce potter, ten strokes will be sufficient.
29. Centrifuge mitochondrial suspension at 15,000 × *g* for 10 min at 4 °C.
30. Discard the supernatant and resuspend gently the mitochondrial pellet in homogenization buffer for western blot analysis, adding the protease and phosphatase inhibitor cocktails, then store the mitochondria fraction at −20 °C.
31. The quality of preparations will be checked by western blot, using different markers for a single fraction, to exclude the presence of contamination. Mitochondrial proteins and cytoskeleton proteins will be used as specific markers for mitochondrial and cytosolic fraction, respectively. For the protocol of western blot, please refer to Subheading 4.1.2.

3.2.3 Data Handling/ Processing

Excluded the presence of contaminations in the cytosolic and mitochondrial fractions, the intracellular redistribution to mitochondria of mitophagic markers, such as OPTN, NDP52, parkin, and PINK1, will be analyzed. In resting condition, these mitophagic markers are expressed in the cytoplasm, their redistribution and accumulation to mitochondrial fraction indicates the activation of mitophagic response (Fig. 5).

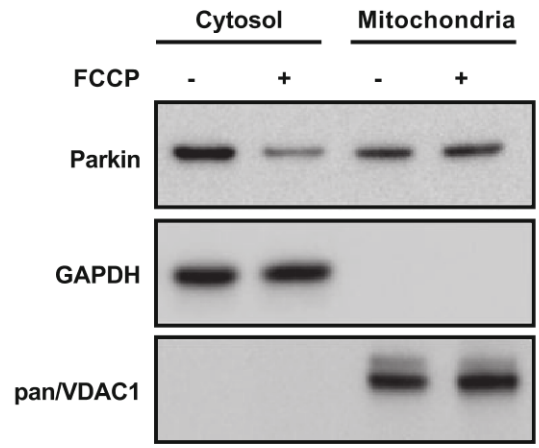

Fig. 5 Parkin translocation by subcellular fractionation. Parkin localization at the mitochondria was assessed by immunoblot after subcellular fractionation. Following treatment with the mitochondrial uncoupler FCCP, Parkin relocates from cytosolic to the mitochondrial fractions. GAPDH and pan/VDAC1 were used as cytosolic and mitochondrial markers, respectively

3.2.4 Notes

1. BSA is essential to bind and remove free fatty acids.
2. It is important to use sucrose containing low-Ca^{2+} contamination. Ca^{2+} contamination can provoke swelling of the mitochondria.
3. Prepare all buffers freshly on the day of the experiment to avoid sample alteration.
4. High force and speed during homogenization with pestle should be avoided to preserve mitochondria integrity.

3.3 Detecting and Quantifying Mitophagy in Human Body Fluids

Biomarkers can be assumed as multifaceted reporters of healthy status or pathological disorders. Typically, they help to evaluate prognosis or disease risk, to guide clinical diagnosis and to monitor individual response to treatment. Up to now, few studies have investigated the possibility of using mitophagy-related proteins as diagnostic and monitoring biomarkers for the most common human diseases. Recently, we demonstrated that both autophagic and mitophagic elements are present in human body fluids of patients affected by neurodegenerative disorders [88–90]. Most interestingly, in these studies, we demonstrated that the levels of mitophagic elements were related to the inflammatory status of the patient and the active/inactive state of the investigated disease. Considering this aspect, monitoring mitophagy by detecting its essential component in several body fluids of affected patients may be of critical importance.

The ELISA is a well-established approach to test the presence of one or more antigens in a sample. Usually, for capturing the analyte to be measured, an antigen-specific antibody is precoated

onto the bottom of the well. Then, a complex will form when the detection antibody (with biochemical modifications that can vary among manufacturers) and the enzyme substrate are added to the wells. This will produce a visible signal correlated to the amount of the analyte(s) present in the sample.

ELISA assay is able to determine circulating levels of proteins involved in the mitophagic pathway such as Parkin, PINK1, OPTN, and NDP52 (CALCOCO2) from human body fluids and with great sensitivity (Parkin: 1 pg/ml and 0.1 ng/ml for PINK1, OPTN, and NDP52), high detection range (Parkin: 1–5000 pg/ml; NDP52: 0.1–10 ng/ml; OPTN: 0.25–8 ng/ml, and for PINK1: 0.625–20 ng/ml), and excellence specificity with no significant cross-reactivity among protein analogs.

3.3.1 Materials

1. Human Parkinson disease 2/parkin (PARK2) ELISA kit, (MyBioSource, MBS732278 or similar).
2. Human serine/threonine-protein kinase PINK1, mitochondrial (PINK1) ELISA kit, (MyBioSource, MBS9327222 or similar).
3. Human optineurin (OPTN) ELISA kit, (MyBioSource, MBS069530 or similar).
4. Human calcium binding and coiled coil domain containing protein 2 (CALCOCO2) ELISA kit, (MyBioSource, MBS7220182 or similar).
5. Human Samples: serum and plasma, possible use of other biological fluids (saliva, urine, feces).
6. Refrigerated centrifuge.
7. Microplate reader (wavelength: 450 nm) with a dedicated software (i.e., SkanIt Software, ThermoFisher; SPECTROstar Nano, BMG labtech or compatible).
8. Incubator.
9. Precision single and multichannel pipette.
10. Disposable tips.
11. Clean tubes and Eppendorf tubes.
12. Deionized or distilled water.
13. All materials supplied by each kit.

3.3.2 Methods

Carry out all procedures at RT, unless otherwise specified. Consider the procedure listed below as the same for all ELISA kits proposed, unless otherwise specified.

Sample Collection and Preparation (*see* **Notes 1** and **2**)

1. Serum: Place whole blood sample from 30 min to 2 h or put it at 4 °C overnight and centrifuge for 15 min at approximately 1000 × *g*.

2. Plasma: Collect plasma using EDTA-Na_2 as an anticoagulant. Centrifuge samples for 15 min at 1000 × *g* at 4 °C within 30 min of collection.
3. Other biological fluids (saliva, urine, feces). Centrifuge samples for 20 min at 1000 × *g* at 4 °C (*see* **Notes 1** and **2**).
4. Collect supernatant from 1–3 steps and estimate the concentration of target protein in the assay by making preexperiment readings. Then, select a proper dilution factor so that protein concentration falls in the optimal range of detection provided by the manufacturer. Dilution of the sample should be performed with the dilution buffer of the kit or PBS (pH 7.0–7.2) (*see* **Notes 3** and **4**).

Reagents Preparation.
Bring all components of the kit at RT before use.

5. Wash buffer. Dilute 10 ml of the provided wash buffer into 990 ml deionized or distilled water, mix gently. Solution can be stored at 4 °C.
6. Other components are ready to use (included standards).

Assay Procedure (*see* **Notes 5** and **6**)

1. Aliquot 0.1 ml of standards (in the case of PINK1 and OPTN, 0.05 ml) into the standard wells (*see* **Note 7**).
2. Aliquot 0.1 ml of PBS (pH 7.0–7.2) into the control well.
3. Aliquot 0.1 ml of diluted (or undiluted) sample (in the case of PINK1 and OPTN, 0.05 ml) into sample test wells (*see* **Notes 2** and **7**).
4. Aliquot 0.01 ml of balance solution into sample test wells only and mix well (if the sample is serum or plasma, this step could be skipped for both kits).
5. Add 0.05 ml of conjugate (in the case of PINK1 and OPTN, 0.1 ml) to each well (not to the control one) and mix well.
6. Cover the plate with a coverslip and incubate at 37 °C for 60 min.
7. Remove the coverslip and discard standards, control, and samples.
8. Wash the plate five times with 0.3 ml wash buffer.
9. Add 0.05 ml substrate A plus 0.05 ml substrate B to each well (*see* **Notes 1** and **8**).
10. Seal the plate with a coverslip and incubate at 37 °C for 15–20 min (*see* **Note 9**).
11. Add 0.05 ml stop solution into each well and mix them (*see* **Note 1**).
12. Read the optical density (O.D.) at 450 nm in a microplate reader immediately after the stop solution.

3.3.3 Data Analysis

Set up the software of the microplate reader in order to:

1. Shake gently (5–10 s) the plate before acquisition.
2. Acquire absorbance for all experimental wells.
3. Calculate the average of duplicate readings for standards, control, and samples.
4. Subtract the average control O.D. from all other well readings before result interpretation.
5. Make a standard curve by plotting the average standard O.D. on the Y-axis against the concentration on the X-axis and draw a best fit curve using (if possible) a four parameter logistic (4-PL) method for Parkin and NDP52 detection and a linear curve fitting for PINK1 and OPTN measurements (Fig. 6) (*see* **Note 10**).

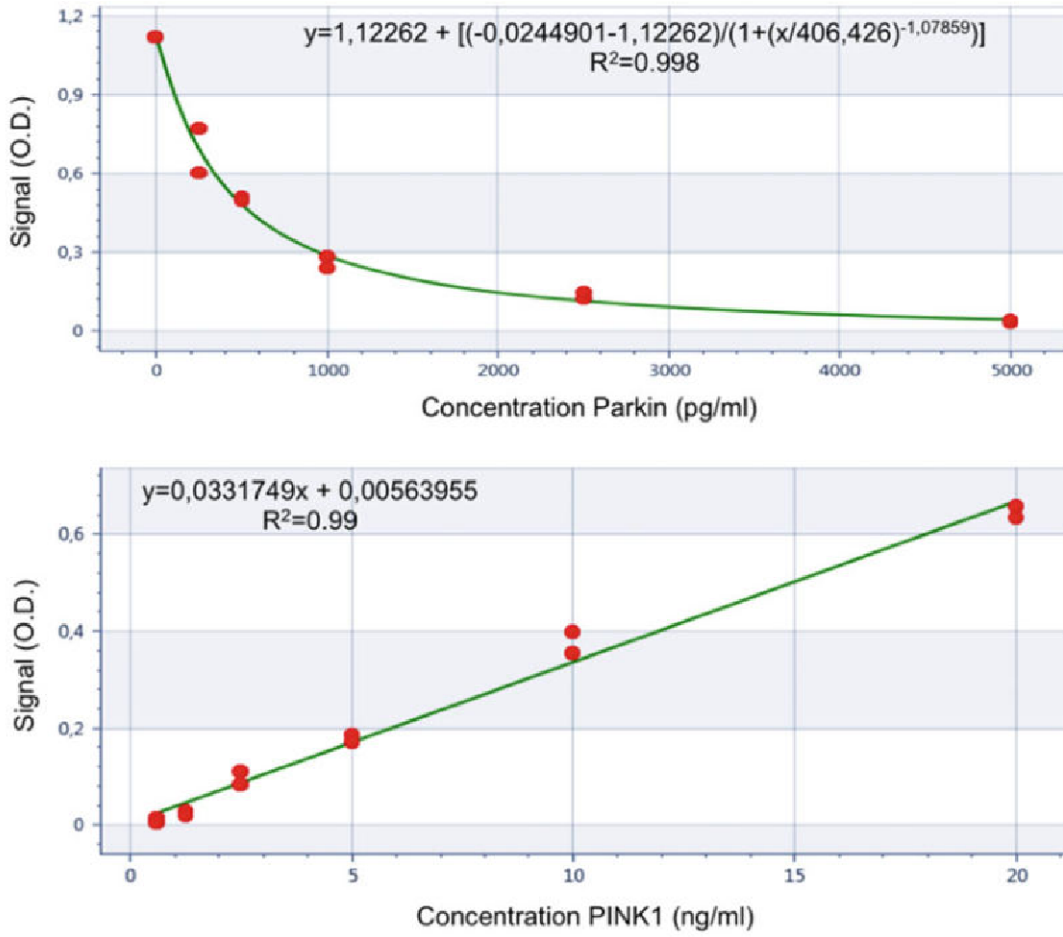

Fig. 6 Detecting and quantifying mitophagy in human body fluids Representative standard curve with a four parameter logistic (4-PL) method for Parkin detection (upper panel) and a linear curve fitting for PINK1 measurements (lower panel)

6. Calculate samples concentration in pg/ml (Parkin) or in ng/ml (PINK1, OPTN, and NDP52) on the basis of the standard curve equation (*see* Figs. 1 and 2 as example) and multiply by the dilution factor (*see* **Note 9**).

3.3.4 Notes

1. Substances provided in the kit may be hazardous in case of skin and eye contact or inhalation. Be careful and wear gloves.
2. All blood components and biological materials should be handled as potentially hazardous.
3. The manufacturer and we suggest preexperiments with the following conditions: undiluted samples, diluted 1:2 and 1:4.
4. Samples should be frozen if not immediately analyzed; in that case, avoid also multiple freeze-thaw cycles.
5. Cover all kit components and store at 4 °C when not in use.
6. Do not use reagents after the kit expiration date.
7. It is recommended that all conditions are run in duplicate.
8. TMB is light-sensitive, please avoid exposure to light.
9. At the end of the procedure if the color is not dark, you can prolong the incubation time until 30 min.
10. Coefficient of determination of the standard curve should be ≥ 0.98.

4 Measuring the Mitochondrial Balance

Mitochondria are the main site for diverse biochemical processes, including the Krebs cycle [91], β-oxidation of fatty acids [92], oxidative phosphorylation [93], and Ca^{2+} homeostasis [94, 95]. To accomplish these physiological processes, mtDNA, lipids, and proteins occasionally become damaged and must be repaired. A large number of cellular pathways are involved to maintain their normal function and provide an efficient quality control system. During these events, mitochondria undergo several rearrangements, in particular in their morphology, functions, and metabolism [96]. To monitor, these dynamics represent a fundamental aspect of understanding the molecular mechanisms involved in the mitochondrial quality control system. Following, we will describe the main methods to assess parameters of mitochondrial function, metabolism, morphology, and protein damage.

4.1 Assessment of the Mitochondrial Structures

It is widely accepted that the fragmentation of the mitochondrial network represents the most common event following a stress condition. This parameter can be detected by measuring the length of a cell's mitochondrial population. Fluorescent microscopy represents the main method to image the mitochondrial network and fragmentation events. This information can be obtained by

transfecting cells with plasmids that present a mitochondrial target sequence. The most used are the mitochondrially targeted green fluorescent protein (mtGFP) plasmid [96] and the red fluorescent protein mCherry-Mito7 [80].

4.1.1 Materials

1. Biological material (cell cultures of interest).
2. Culture medium Dulbecco's Modified Eagle Medium (DMEM; e.g., Gibco 11965084) supplemented with 10% FBS, 1% penicillin-streptomycin, and 1% L-glutamine.
3. 1× PBS buffer, pH 7.4, no phenol red. In 1 l of distilled water, add 8 g of NaCl, 0.2 g of KCl, 1.44 g of Na_2HPO_4, 0.24 g of KH_2PO_4. Adjust the pH to 7.4 with HCl.
4. Appropriate transfection reagent (e.g.; Lipofectamine LTX with Plus Reagent, ThermoFisher, 15338100).
5. mtGFP.
6. Glass coverslips 24 mm in diameter.
7. Six-well culture plates.
8. 4% PFA solution, pH 7.4, in 1× PBS. Add 4 g of PFA in 100 ml of 1× PBS.
9. Inverted Nikon confocal microscope system A1 R.

4.1.2 Methods

Sample Preparation and Transfection

1. Plate cells on glass coverslips at a density of 100,000 cells.
2. When cells reached a confluence of 50–60%, transfect them with 500 ng mtGFP plasmid by using the appropriate method (*see* **Note 1**).
3. After 4–6 h, replace the transfection medium with warm medium culture.
4. After 24 h, image the cells. Alternatively, cells can be fixed in 4% PFA for 15 min at RT, washed three times with 1× PBS, and stored at 4 °C in the dark (*see* **Note 2**).

Measurement:

5. Move the coverslips into a cell chamber and place in a 37 °C thermo-controlled stage of the inverted confocal microscope system.
6. Capture picture at high-resolution by using standard binning mode 1 × 1 (meaning that each logical pixel is equal to one physical pixel) and collect a z-stack series of images at 0.2–0.5 μm each, to capture the whole mitochondrial network of the cell (*see* **Note 3**).
7. To obtain a statistical measurement of the mitochondrial network, acquire at least 20–25 images per condition and store images.

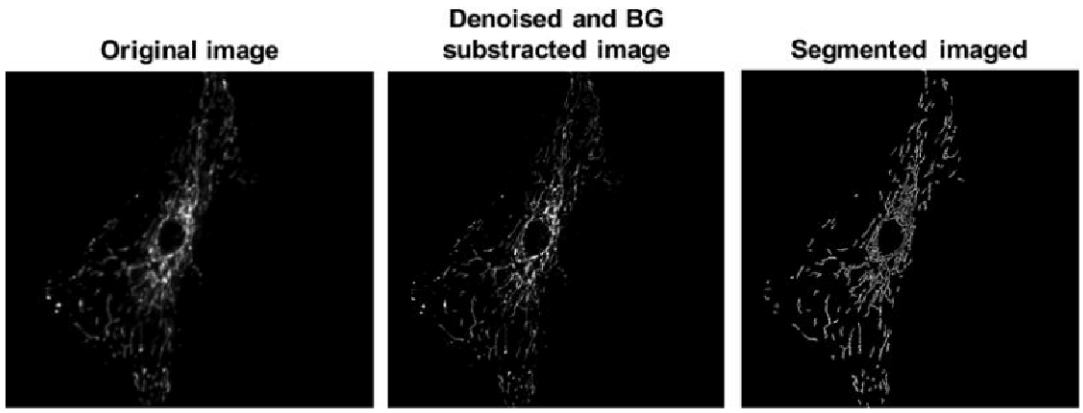

Fig. 7 Assessment of the mitochondrial structures. Representative images showing the mitochondrial network derived from mtGFP-expressing cells. Left panel represents the volume rendering of a cell before denoising and subtraction of background (BG, middle panel). The right panel depicts the segmented image generated by the 3D objects counter plug-in installed in Fiji software

4.1.3 Data Handling/ Processing

The analysis of mitochondrial morphology may be achieved directly with the microscope imaging software or by using open-source software programs such as Fiji software (Fig. 7). We suggest using the plug-in 3D objects counter installed in the open-source Fiji software. An automated algorithm will calculate the average volume of mitochondria, the total volume, and the number of mitochondria counted for each cell. Before running the 3D objects counter plug-in, we recommend to denoise images by applying a Gaussian filter (Menu→Filters→Gaussian...) and remove the background setting the rolling ball to a size of 1 um (Menu Process → Substract background...) (*see* **Note 4**).

4.1.4 Notes

1. Primary cell cultures are "hard to transfect" and alternative methods to transfection are needed. A large series of mitochondrial-specific fluorescent dyes (MitoTracker Green, MitoTracker Orange, MitoTracker Red, and MitoTracker Deep Red) may be used to stain the mitochondrial structures of primary cell samples. Please remember that these chemical fluorescent dyes are sensitive to alteration in mitochondrial membrane potential.
2. Several fixation methods are reported to alter mitochondrial structures. We recommend to fix cells with 4% PFA.
3. Attenuate laser excitation potency to minimize photobleaching and photodamage and keep constant camera settings and illumination across samples.
4. The background subtraction should not be modified between samples.

4.2 Assessing Changes in Mitochondrial Functioning by Immunoblot of Mitochondrial Complexes

The method described in Subheading 4.1 is a useful approach to investigate the mitochondrial amounts by immunoblot. Despite this, it cannot provide information about the functionality of mitochondria. This can be done by measuring the levels of all five mitochondrial complexes of the electron transport chain (ETC). Notably, dysfunction in mitochondrial ETC compromises ATP production and accelerates the generation of free radicals. To evaluate the mitochondrial ETC function, the conventional methods used are spectrophotometric assays and blue native polyacrylamide gel electrophoresis (BN-PAGE) [97]. Alternatively, the protein complexes can be assessed by using commercially antibody cocktails that probe for all five complexes at once.

4.2.1 Materials

1. Biological material (cell cultures of interest).
2. Culture medium Dulbecco's Modified Eagle Medium (DMEM; e.g., Gibco 11965084) supplemented with 10% FBS, 1% penicillin-streptomycin, and 1% L-glutamine.
3. RIPA lysis buffer (150 mM sodium chloride, 1.0% NP-40 or Triton X-100, 0.5% sodium deoxycholate, 0.1% SDS, 50 mM Tris, pH 8.0, supplemented of protease and phosphatase inhibitor).
4. CAPS-based transfer buffer (10 mM CAPS, pH 11, 10% methanol) (*see* **Note 1**).
5. Tris-buffered saline (TBS; 10×): 1.5 M NaCl, 0.1 M Tris–HCl, pH 7.4.
6. TBS containing 0.05% Tween-20 (TBS-T).
7. Blocking Solution: 5% milk in TBS-T.
8. Precast gel 4–12% Bis-Tris bolt (ThermoFisher, NW04120BOX).
9. PVDF membranes.
10. Primary antibody anti-OXPHOS (*see* **Notes 2** and **3**).
11. Primary antibody anti-GAPDH.
12. Restore western blot stripping buffer (ThermoFisher, 21059).

4.2.2 Methods

Sample Preparation and Homogenates Collection

1. Plate cells in 6-well plates at a density of 150,000 cells.
2. After at least 24 h, cellular homogenates are collected and lysed by using RIPA lysis buffer. Keep homogenates in ice and vortex them every 5 min.
3. After 30 min, centrifuge cell lysates at 12,000 × *g* for 10 min at 4 °C, collect the supernatant, and keep them at −80 °C.

Western Blot for OXPHOS Components

4. After having determined the protein concentration for the cell lysate, prepare 10–15 μg of each the sample in nondenaturating conditions. To avoid unspecific aggregation of the proteins, we recommend to do not boil the samples before.
5. Load samples in a precast gel 4–12% and perform the electrophoresis at 150 mV for 30–45 min.
6. Following electrophoresis, activate PVDF with methanol for 1 min and rinse with transfer buffer. Assemble the transfer stack with sponges, filter papers, PVDF membrane, and gel, being careful to that the gel is facing the cathode (−) and the membrane side is facing the anode (+). We recommend to transfer the gel for 2 h at 350 mA.
7. After the protein transfer, rinse the membrane in TBS-T and place the membrane in blocking solution and incubate with agitation for 1 h.
8. Place the blot in the primary antibodies solution (*see* **Note 4**) and incubate with agitation overnight. Wash the blot three times for 5 min.
9. Place the blot in the secondary antibody solution and incubate with agitation for 1 h at RT. Wash the blot three times for 5 min.
10. Proceed with chemiluminescent detection.

Western Blot for Loading Marker

11. After detection, wash blot to remove chemiluminescent substrate.
12. Incubate blot in Restore western blot stripping buffer for 15 min at RT.
13. Wash the blot three times in TBS-T with agitation for 10 min at RT.
14. Place the membrane in blocking solution and incubate with agitation for 1 h.
15. Place the blot in the primary antibodies solution and incubate with agitation O.N. Wash the blot three times for 5 min.
16. Place the blot in the secondary antibody solution and incubate with agitation for 1 h at RT. Wash the blot three times in TBS-T with agitation for 10 min at RT.
17. Proceed with chemiluminescent detection (Fig. 8).

4.2.3 Data Handling/ Processing

Quantify the bands with a densitometric program (*see* **Note 5**) and then divide to the protein amounts of each complex with the loading marker. In the case two or more cellular conditions are analyzed, we suggest to normalize the values obtained with a mitochondrial marker, to calculate the quantities of the different proteins accordingly to the mitochondrial amounts.

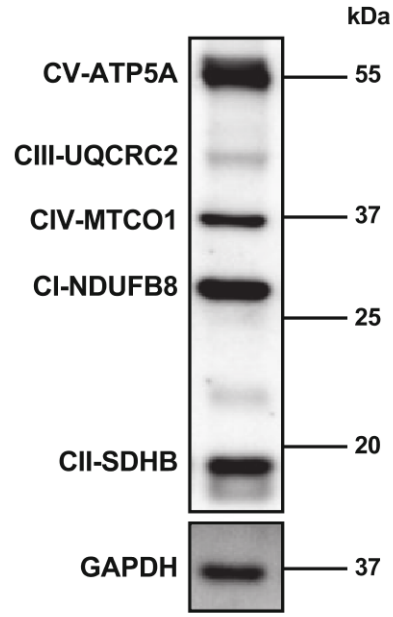

Fig. 8 Assessing changes in mitochondrial functioning by immunoblot of mitochondrial complexes. Levels of mitochondrial electron transport chain complex proteins were analyzed by western blot of extracts (samples mixed with sample buffers at room temperature for 10 min without boiling) from primary cortical neurons by using abcam's total OXPHOS rodent antibody cocktail

4.2.4 Notes

1. 10 mM CAPS Buffer pH: 11 will facilitate the protein migration in an electric field. Alternatively, use a lower pH buffer such as an acetic acid buffer.
2. This can be done individually by purchasing separate antibodies and probing each complex individually.
3. All mETC complexes are very sensitive to heating. Be careful to do not heat over 50 °C.
4. The antibody cocktail (1.5 mg/mL) should be diluted 250× to a final working concentration of 6.0 μg/ml for western blotting.
5. COXI band will appear at ~35 kDa and not at its true molecular weight at 57 kDa.

4.3 Assessment of Mitochondrial Function Utilizing Seahorse Extracellular Flux

The metabolic activity of mitochondria may be detected by using the XF96 Extracellular Flux Analyzer (Seahorse Bioscience) [98–101]. By adding specific modulators of respiratory complexes during the assay, this instrument permits to reveal key parameters of mitochondrial function: basal respiration (OCR-basal) that shows the energetic demand of the cell in baseline conditions; ATP-production (OCR-ATP) that shows the ATP produced by

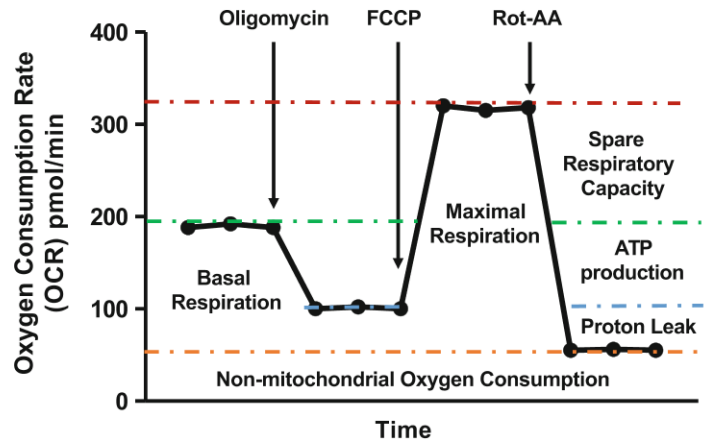

Fig. 9 Assessment of mitochondrial function utilizing Seahorse instrument. Schematic Mito Stress assay showing calculable parameters

mitochondria; maximal respiratory capacity (OCR-MRC) that is indicative of the maximum rate of respiration that the cell can achieve; spare respiratory capacity (SRC-OCR) that represents how the cell responds to an energetic demand (Fig. 9).

To achieve this information, the instrument performs subsequent injections of modulators of respiration into each well during the assay. The modulators are: the inhibitor of ATP synthase (Complex V) oligomycin, which decreases electron flow determining a decrease in OCR; the uncoupling agent FCCP that disrupts mitochondrial membrane potential and provokes an increase in OCR; a mixed solution composed of rotenone and antimycin-A (Rot-AA) that inhibits the Complex-III, resulting in a collapse of the mitochondrial respiration. In the following protocol, we will describe the method to measure the OCR in adherent cells by using the Agilent Seahorse XF Cell Mito Stress Test.

4.3.1 Materials

1. Biological material (cell cultures of interest) (*see* **Note 1**).
2. 1× PBS buffer, pH 7.4, no phenol red. In 1 l of distilled water, add 8 g of NaCl, 0.2 g of KCl, 1.44 g of Na_2HPO_4, 0.24 g of KH_2PO_4. Adjust the pH to 7.4 with HCl.
3. Seahorse XFe96 Analyzer (Agilent Technologies).
4. XFe96 MitoStress Test kit (Agilent Technologies, 103015-100). The kit contains six pouches. Each pouch contains one each of oligomycin, FCCP, and rotenone/antimycin A (Rot-AA) (*see* **Note 2**).
5. Seahorse XF96 cell culture microplates (Agilent Technologies, 101085-004) (*see* **Note 1**).
6. Seahorse XF calibrant (Agilent Technologies, 100840-000).

7. Seahorse XF assay medium modified DMEM (XF DMEM) (Agilent.
8. Technologies, 102365-100).
9. Culture medium Dulbecco's Modified Eagle Medium (DMEM; e.g., Gibco 11965084) supplemented with 10% FBS, 1% penicillin-streptomycin, and 1% L-glutamine.
10. 1 mM sodium pyruvate.
11. 10 mM D-(+)-glucose.
12. 2 mM L-glutamine.
13. 0.1% crystal violet solution.
14. 4% PFA solution, pH 7.4, in 1× PBS. Add 4 g of PFA in 100 ml of 1× PBS.
15. Microplate spectrophotometer.

4.3.2 Method

The Day Before of the Assay:

1. Add 200 µl of Seahorse Bioscience calibrant, pH 7.4, to each well of a Seahorse Bioscience 96-well utility microplate (*see* **Note 3**).
2. Place sensor cartridge on top of the utility plate and store at 37 °C without CO_2 overnight and turn on instrument and start XF software to allow instrument to stabilize at 37 °C.
3. Plate cells in a range of 5×10^4 cells per well in DMEM. We recommend to be sure that in the day of assay, cells are uniformly spread throughout the well.
4. Pipette 200 µl of the cell suspension into each well of 96-well microplate. At least two wells should lack cells to be used as a blank control. Put the seeded plate into a 37 °C, 5% CO_2 incubator to allow cells to grow overnight.

The Day of Assay:

5. Warm XF DMEM media to 37 °C, add 2 mM L-glutamine, 10 mM glucose, and 1 mM sodium pyruvate and adjust the pH of the media to 7.4.
6. Remove all but 25 µl of media from each well and add 175 µl of warm XF DMEM media, pH: 7.4. Place the plate in a 37 °C incubator without CO_2 for 1 h before running an assay.
7. Prepare the inhibitors in XF DMEM media at a concentration of 10x higher than the final dilution. Prepare 3 ml of 15 µM oligomycin, 3 ml of 10 µM FCCP, and 3 ml of 5 µM Rot-AA and add 25 µl of each solution into injection ports A, B, and C, respectively. Fill also A, B, and C injection ports of blank wells (*see* **Note 4**).

8. Running the assay with the desired protocol. The XF96 analyzer required an input protocol composed of mix time, wait, and measure time. We suggest using a protocol composed of 3-min mix time, 3-min wait time and 3-min measure time for each point.
9. After the assay, the OCR data should be normalized to cell number or protein concentration. We suggest quantifying cell number by using crystal violet method. Fix cells with 4% PFA for 15 min at RT and stain cells with a 1% crystal violet solution for 15 min at RT. Measure the absorbance at 595 nm by using a microplate reader (*see* **Note 5**).

4.3.3 Data Handling/ Processing

OCR-Basal, OCR-ATP, OCR-MRC, and OCR-SRC can be calculated by using the following equations:

1. Basal Respiration: (Last rate measurement before first injection)—(nonmitochondrial respiration rate).
2. Maximal Respiration: (Maximum rate measurement after FCCP injection)—(nonmitochondrial respiration).
3. ATP Production: (Last rate measurement before oligomycin injection)—(minimum rate measurement after oligomycin injection).
4. Spare Respiratory Capacity: (Maximal respiration)—(basal respiration).

Further parameters can be calculated:

5. H+ (Proton) Leak: (Minimum rate measurement after oligomycin injection)—(nonmitochondrial respiration).
6. Non-mitochondrial Oxygen Consumption: Minimum rate measurement after Rot-AA injection (Fig. 10).

H+ Leak represents the remaining basal respiration not coupled to ATP production and can be related to mitochondrial damage. Non-mitochondrial respiration may indicate the existence of subcellular enzymes that consume oxygen after the third injection of Rot-AA.

4.3.4 Notes

1. Bioenergetic information can be also assessed in isolated mitochondria and in nonadherent cells.
2. The protocol outlined here is for the 96-well format of the instrument. Volumes will need to be adjusted if another format is used.
3. Verify that the calibrant solution level is high enough to keep the sensors submerged.
4. Each series of ports (e.g., all ports A) must contain the same volume.

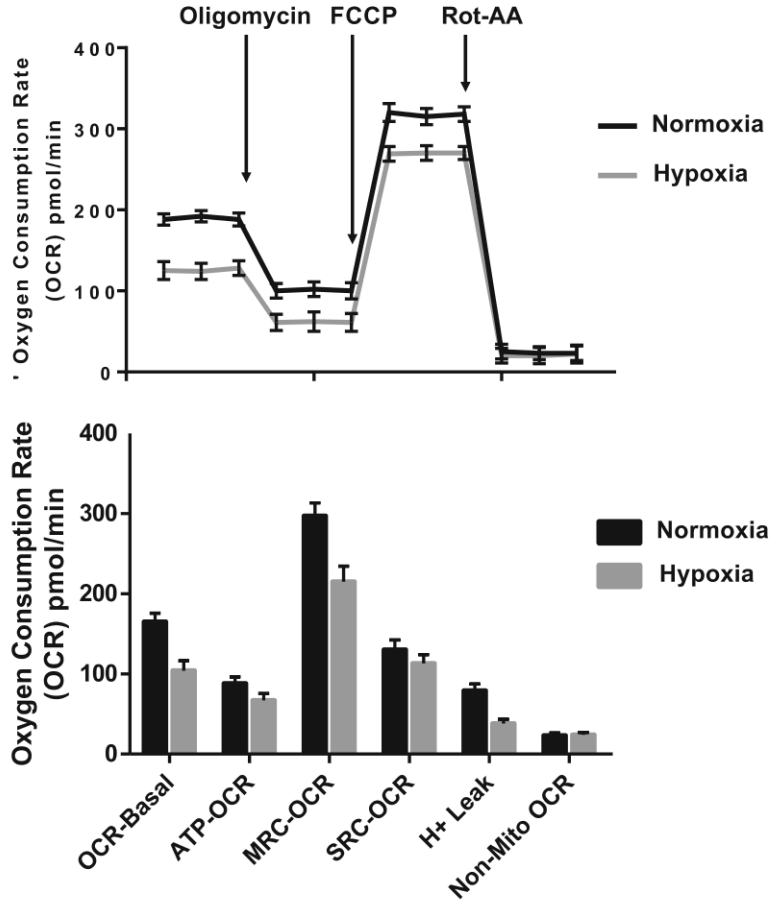

Fig. 10 Oxygen consumption rate (OCR) in Mito Stress assay. Oxygen consumption rate (OCR) assessed in primary cells exposed to hypoxic condition. To perform these experiments, before measurements cells were incubated with a solution 50 μM cobalt (III) chloride hexahydrate ($CoCl_2$). OCR was measured under basal condition and following perfusion of oligomycin, FCCP, and Rot-AA. Each data point represents an OCR measurement performed in at least three different wells of a 96-well plate. The graphs are representative of the calculated parameters for basal respiration (OCR-basal), ATP production (ATP-OCR), maximal respiration (MRC-OCR), spare respiratory capacity (SRC-OCR), proton leak (H + Leak), and non-mitochondrial respiration (non-mito OCR)

5. If it is not convenient to proceed with the protein concentration assay, it is possible to freeze the whole plate at −20 °C until analysis.

4.4 Monitor Mitochondrial Turnover with MitoTimer

First efforts to measure mitochondrial turnover were performed in late 1950s by monitoring 35S-methionine incorporation into newly synthesized proteins [102]. Newly, a protocol describes the possibility to measure the changes of mitochondrial proteins by using deuterium labeling and mass spectrometry [103]. The main

limitation of these methods is the impossibility to imaging the process. To visualize mitochondrial turnover, the fluorescent Timer construct (DsRed1-E5) has been recently targeted to the mitochondrial matrix by fusing the mitochondrial targeting sequence of the COX8A subunit [104]. The main characteristic of Timer is to shift its fluorescence overtime from green to red as the protein matures. In view of this, different information can be achieved by using this novel construct:

1. Increases in red signal without changes in green channel may suggest impairments in mitochondrial degradation.
2. The newly synthesized mitochondria appear green-only.
3. Yellow mitochondria are indicative of an intermediate stage of mitochondria and represent the fusion process of newly synthesized (green) and old/mature (red) mitochondria.

4.4.1 Materials

1. Biological material (cell cultures of interest).
2. Culture medium Dulbecco's Modified Eagle Medium (DMEM; e.g., Gibco 11965084) supplemented with 10% FBS, 1% penicillin-streptomycin, and 1% L-glutamine.
3. 1× PBS buffer, pH 7.4, no phenol red. In 1 l of distilled water, add 8 g of NaCl, 0.2 g of KCl, 1.44 g of Na_2HPO_4, 0.24 g of KH_2PO_4. Adjust the pH to 7.4 with HCl.
4. 4% PFA solution, pH 7.4, in 1× PBS. Add 4 g of PFA in 100 ml of 1× PBS.
5. Transfection reagent (Lipofectamine LTX with Plus Reagent, ThermoFisher, 15338100).
6. Mitochondrial fluorescent Timer construct (MitoTimer).
7. Glass coverslips.
8. Six-well culture plates.
9. Cell chamber (Attofluor cell chamber, ThermoFisher, A7816).
10. Inverted Zeiss LSM 510 confocal microscope (*see* **Note 1**).

4.4.2 Methods

Sample Preparation and Transfection

1. Plate cells onto coverslips (24 mm in diameter) at a density of 100,000 cells per coverslip.
2. When cells reached a confluence of 50–60%, transfect them with 1 μg/coverslips of MitoTimer plasmid by using the appropriate method.
3. After 4–6 h, replace the transfection medium with warm medium culture, and after 24 h cells image the cells. Alternatively, cells can be fixed in 4% PFA for 15 min at RT, washed three times with 1× PBS, and stored at 4 °C in the dark (*see* **Note 2**).

4. Move the coverslips into a cell chamber and place in a 37 °C thermo-controlled stage of the inverted Zeiss LSM 510 confocal microscope (*see* **Note 3**). Fluorescence images were captured providing excitation at 488 nm (green) and 546 nm (red) with detection of green (500–540 nm) and red (580–640 nm) fluorescence signals (*see* **Note 4**).
5. To obtain a statistical measurement of the mitochondrial network, acquire at least 20–25 images per condition (*see* **Note 5**).

4.4.3 Data Handling

Image processing may be achieved by using the microscope software (ZEN elements for Zeiss instruments) or Fiji software. After background subtraction on both green and red channel, ratiometric images were generated, and the quantification of red/green ratio signal was performed by registering the mean pixel intensity. To quantify the yellow signal, we suggest to use the colocalization plug-in available in Fiji software or the colocalization command of ZEN software (Fig. 11).

4.4.4 Notes

1. MitoTimer is also suitable for analysis by flow cytometry using a 488 nm laser for excitation and detection in the FITC and PE channels.
2. Sample transfected with MitoTimer can be fixed. In addition, fixation prevents postfixation maturation and stabilizes green and red conformations.
3. Changes in temperature may provoke transition from green to red fluorescence. It is recommended to use a 37 °C thermo-controlled stage during imaging.
4. Prolonged light exposure during live-cell imaging may accelerate the maturation (red photoconversion). Keep laser potency and exposure time low.
5. Keep exposure time and illumination constant across samples.

4.5 Monitor Mitochondrial Energetic Levels with Fluorescent Probes

Among the different major events that occur in mitochondria during damage/stress condition, the loss of mitochondrial transmembrane potential ($\Delta\Psi_m$) is the most significant [105]. This force is generated by proton pumps (C-I, III, and IV of mitochondrial ETC), and together with the proton gradient (ΔpH) is the central mitochondrial parameter that regulates ATP, synthesis, respiratory rate, and production of ROS. In addition to this, $\Delta\Psi_m$ represents the driving force that regulates the transport of different charged compounds (such as Ca^{2+}) [106], and its dissipation determines the activation of the mitophagic pathway regulated by PINK1-Parkin axis. Several fluorescent probes are used to investigate the levels of $\Delta\Psi_m$. Among them, the most used are fluorescent cationic dyes including rhodamine 123 (Rh123), JC1, tetramethylrhodamine ethyl (TMRE) or methyl (TMRM) ester, nonyl acridine orange

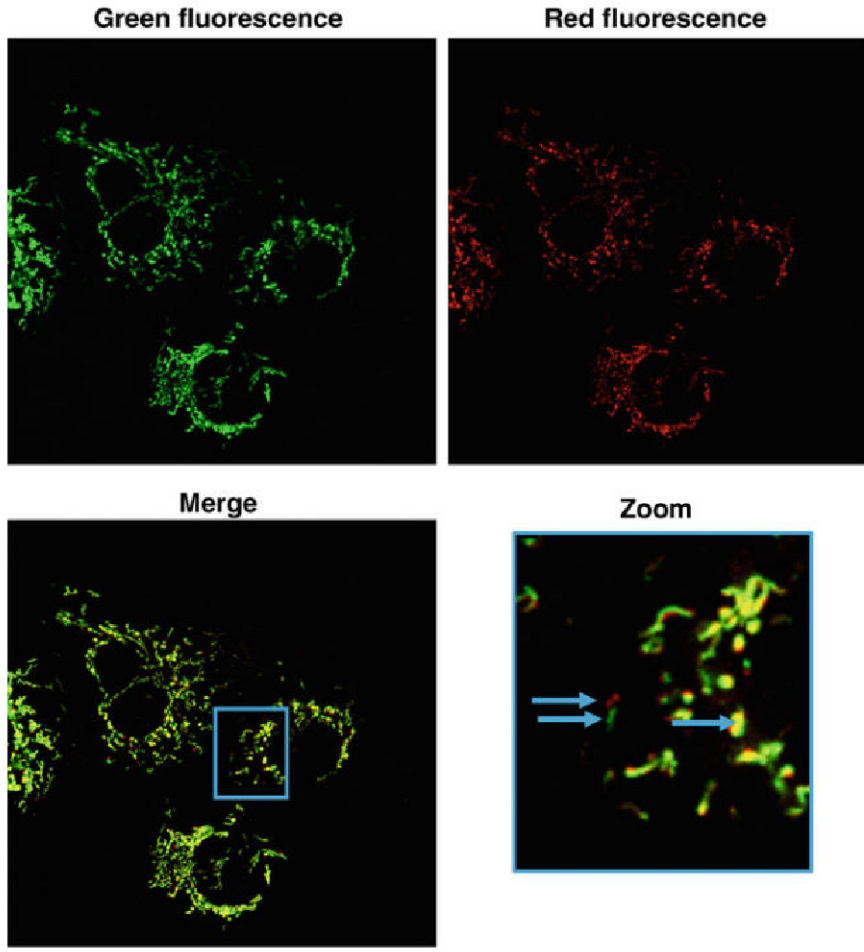

Fig. 11 Monitor mitochondrial turnover with MitoTimer. Fluorescent images of MitoTimer expressing cells. Red-only mitochondria are representative of old mitochondria. Green-only mitochondria represent newly synthesized mitochondria. Yellow staining depicts an intermediate stage of mitochondria

(NAO), and merocyanine 540 [107]. From first glance, JC1 may represent the best opportunity due to the fact that this probe forms red-fluorescent aggregates in low-potential mitochondria or green-fluorescent aggregates in mitochondria characterized by high-potential. At the same time, this probe has diverse adverse effects like photodamage and changes of fluorescence independent from $\Delta\Psi_m$. In light of this, we suggest using TMRM or TMRE to monitor variation in $\Delta\Psi_m$. This cell-permeable fluorescent indicator accumulates in the mitochondrial matrix in proportion to $\Delta\Psi_m$, and compared to other probes, this has limited effect on mitochondrial respiration as well as low photobleaching and phototoxicity [108, 109].

4.5.1 Materials

1. Biological material (cell cultures of interest).
2. Culture medium Dulbecco's Modified Eagle Medium (DMEM; e.g., Gibco 11965084) supplemented with 10% FBS, 1% penicillin-streptomycin, and 1% L-glutamine.
3. 1× PBS buffer, pH 7.4, no phenol red. In 1 l of distilled water, add 8 g of NaCl, 0.2 g of KCl, 1.44 g of Na_2HPO_4, 0.24 g of KH_2PO_4. Adjust the pH to 7.4 with HCl.
4. Tetramethylrhodamine, TMRM (ThermoFisher, T668).
5. 10 mM FCCP.
6. Glass coverslips (24 mm in diameter).
7. Six-well culture plates.
8. Cell chamber (Attofluor cell chamber, ThermoFisher, A7816).
9. Inverted Zeiss LSM 510 confocal microscope.

4.5.2 Methods

Sample Preparation

1. Plate cells on glass coverslips (24 mm in diameter) a density of 150,000 cells. After seeding the cells, wait for at least 24 h (*see* **Note 1**).
2. Wash cells with prewarmed 1× PBS and incubate cells with TMRM in the appropriate cellular media at 37 °C for 30 min. We recommend to use low concentration of the probe (10–25 nM range) to avoid autoquenching (*see* **Note 2**).
3. Move the coverslips into a cell chamber.
4. Place the coverslip on a stage incubator of the confocal microscope equipped with a high magnification objective (*see* **Notes 3** and **4**).
5. Once having adjusted the focus of the cells using reflected light and examine TMRM fluorescence by excitation at 515 nm and emission at 595 nm, collect images with time-lapse interval of 50 or 200 ms image acquisition/illumination time for 1 min to register the basal TMRM fluorescent intensity.
6. Apply a stimuli 1 μM FCCP, which will depolarize the $\Delta\Psi_m$. These changes provoke a decrease in TMRM fluorescence intensity and will be indicative of background fluorescent intensity of TMRM. Record images for 1 min (*see* **Note 5**).

4.5.3 Data Handling Analysis

Data analysis should be achieved by using the ROI tool from the microscope program or from Fiji. Select ROIs from mitochondrial regions and calculate the average fluorescence intensities. Subtract the average fluorescent intensity after FCCP addition from average basal fluorescent intensity of TMRM. Then, use Prism or Excel program to generate the graphs and plots indicative of changes in fluorescence intensity overtime (Fig. 12).

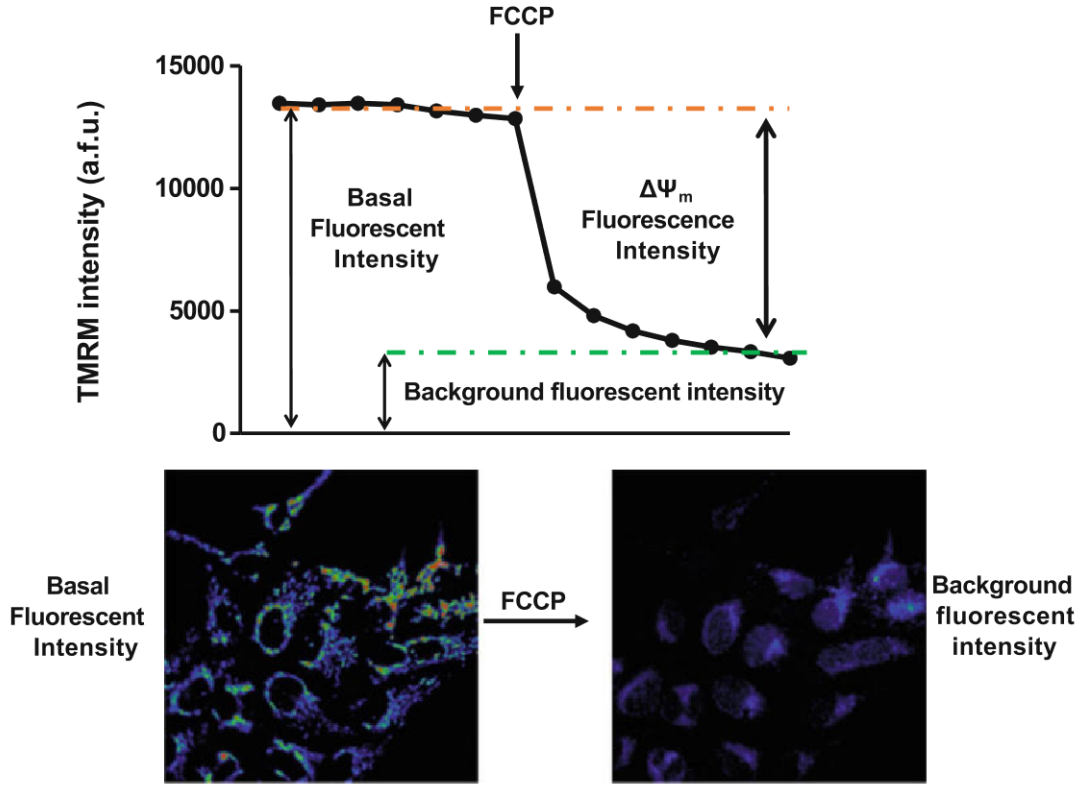

Fig. 12 Monitor mitochondrial energetic levels with fluorescent probes. Representative trace of TMRM fluorescence signal showing calculable parameters. After registering the basal fluorescence intensity, FCCP was added to collapse the mitochondrial membrane potential ($\Delta\Psi_m$) and obtain the background fluorescent intensity. Images of fluorescence confocal microscopy of cells loaded with TMRM before and after FCCP addition

4.5.4 Notes

1. At low concentrations of mitochondria, the greater fraction of TMRM remains in the media. In this case, the method may be less sensitive to detect changes in $\Delta\Psi_m$. A mitochondrial protein concentration >1 mg/ml is predicted to be optimal for TMRM assay [108].
2. TMRM staining must not be washed out.
3. Changes in temperature may provoke transition from green to red fluorescence. It is recommend to use a 37 °C thermocontrolled stage during imaging.
4. We suggest to use a 40x magnification to capture an optimal number of cells and to keep laser excitation at low potency to minimize photobleaching and photodamage.
5. Keep exposure time and illumination constant across samples.

Acknowledgments

PP is grateful to Camilla degli Scrovegni for her continuous support. All authors thank the Associazione Ricerca Oncologica Sperimentale Estense (A-ROSE).

Funding: PP was supported by Telethon (GGP15219/B), the Italian Association for Cancer Research (AIRC: IG- 23670), and by local funds from the University of Ferrara. CG was supported by local funds from the University of Ferrara, the Italian Association for Cancer Research (AIRC: IG19803), the Italian Ministry of Health (GR-2013-02356747), and European Research Council Grant 853057-InflaPML. SP was supported by Fondazione Umberto Veronesi.

References

1. Patergnani S, Missiroli S, Marchi S, Giorgi C (2015) Mitochondria-associated endoplasmic reticulum membranes microenvironment: targeting Autophagic and apoptotic pathways in cancer therapy. Front Oncol 5:173
2. Giorgi C, Missiroli S, Patergnani S, Duszynski J, Wieckowski MR, Pinton P (2015) Mitochondria-associated membranes: composition, molecular mechanisms, and physiopathological implications. Antioxid Redox Signal 22:995–1019
3. Giorgi C, Danese A, Missiroli S, Patergnani S, Pinton P (2018) Calcium dynamics as a machine for decoding signals. Trends Cell Biol 28:258–273
4. Pinton P, Leo S, Wieckowski MR, Di Benedetto G, Rizzuto R (2004) Long-term modulation of mitochondrial Ca2+ signals by protein kinase C isozymes. J Cell Biol 165:223–232
5. Shimizu S (2019) Organelle zones in mitochondria. J Biochem 165:101–107
6. Saha PP, Vishwanathan V, Bankapalli K, D'Silva P (2018) Iron-sulfur protein assembly in human cells. Rev Physiol Biochem Pharmacol 174:25–65
7. Jiang S, Park DW, Stigler WS, Creighton J, Ravi S, Darley-Usmar V, Zmijewski JW (2013) Mitochondria and AMP-activated protein kinase-dependent mechanism of efferocytosis. J Biol Chem 288:26013–26026
8. Gomes LC, Di Benedetto G, Scorrano L (2011) During autophagy mitochondria elongate, are spared from degradation and sustain cell viability. Nat Cell Biol 13:589–598
9. Liu L, Feng D, Chen G, Chen M, Zheng Q, Song P, Ma Q, Zhu C, Wang R, Qi W et al (2012) Mitochondrial outer-membrane protein FUNDC1 mediates hypoxia-induced mitophagy in mammalian cells. Nat Cell Biol 14:177–185
10. Murakawa T, Yamaguchi O, Hashimoto A, Hikoso S, Takeda T, Oka T, Yasui H, Ueda H, Akazawa Y, Nakayama H et al (2015) Bcl-2-like protein 13 is a mammalian Atg32 homologue that mediates mitophagy and mitochondrial fragmentation. Nat Commun 6:7527
11. Bhujabal Z, Birgisdottir AB, Sjottem E, Brenne HB, Overvatn A, Habisov S, Kirkin V, Lamark T, Johansen T (2017) FKBP8 recruits LC3A to mediate Parkin-independent mitophagy. EMBO Rep 18:947–961
12. Kitada T, Asakawa S, Hattori N, Matsumine H, Yamamura Y, Minoshima S, Yokochi M, Mizuno Y, Shimizu N (1998) Mutations in the parkin gene cause autosomal recessive juvenile parkinsonism. Nature 392:605–608
13. Deas E, Plun-Favreau H, Wood NW (2009) PINK1 function in health and disease. EMBO Mol Med 1:152–165
14. Nuytemans K, Theuns J, Cruts M, Van Broeckhoven C (2010) Genetic etiology of Parkinson disease associated with mutations in the SNCA, PARK2, PINK1, PARK7, and LRRK2 genes: a mutation update. Hum Mutat 31:763–780
15. Corti O, Lesage S, Brice A (2011) What genetics tells us about the causes and mechanisms of Parkinson's disease. Physiol Rev 91:1161–1218
16. Jin SM, Lazarou M, Wang C, Kane LA, Narendra DP, Youle RJ (2010) Mitochondrial

membrane potential regulates PINK1 import and proteolytic destabilization by PARL. J Cell Biol 191:933–942

17. Yamano K, Youle RJ (2013) PINK1 is degraded through the N-end rule pathway. Autophagy 9:1758–1769
18. Deas E, Plun-Favreau H, Gandhi S, Desmond H, Kjaer S, Loh SH, Renton AE, Harvey RJ, Whitworth AJ, Martins LM et al (2011) PINK1 cleavage at position A103 by the mitochondrial protease PARL. Hum Mol Genet 20:867–879
19. Hasson SA, Kane LA, Yamano K, Huang CH, Sliter DA, Buehler E, Wang C, Heman-Ackah SM, Hessa T, Guha R et al (2013) High-content genome-wide RNAi screens identify regulators of parkin upstream of mitophagy. Nature 504:291–295
20. Lazarou M, Jin SM, Kane LA, Youle RJ (2012) Role of PINK1 binding to the TOM complex and alternate intracellular membranes in recruitment and activation of the E3 ligase Parkin. Dev Cell 22:320–333
21. Okatsu K, Oka T, Iguchi M, Imamura K, Kosako H, Tani N, Kimura M, Go E, Koyano F, Funayama M et al (2012) PINK1 autophosphorylation upon membrane potential dissipation is essential for Parkin recruitment to damaged mitochondria. Nat Commun 3:1016
22. Kondapalli C, Kazlauskaite A, Zhang N, Woodroof HI, Campbell DG, Gourlay R, Burchell L, Walden H, Macartney TJ, Deak M et al (2012) PINK1 is activated by mitochondrial membrane potential depolarization and stimulates Parkin E3 ligase activity by phosphorylating serine 65. Open Biol 2:120080
23. Geisler S, Holmstrom KM, Skujat D, Fiesel FC, Rothfuss OC, Kahle PJ, Springer W (2010) PINK1/Parkin-mediated mitophagy is dependent on VDAC1 and p62/SQSTM1. Nat Cell Biol 12:119–131
24. Pickles S, Vigie P, Youle RJ (2018) Mitophagy and quality control mechanisms in mitochondrial maintenance. Curr Biol 28:R170–R185
25. Lazarou M, Sliter DA, Kane LA, Sarraf SA, Wang C, Burman JL, Sideris DP, Fogel AI, Youle RJ (2015) The ubiquitin kinase PINK1 recruits autophagy receptors to induce mitophagy. Nature 524:309–314
26. Saito T, Sadoshima J (2015) Molecular mechanisms of mitochondrial autophagy/mitophagy in the heart. Circ Res 116:1477–1490
27. Tong M, Saito T, Zhai P, Oka SI, Mizushima W, Nakamura M, Ikeda S, Shirakabe A, Sadoshima J (2019) Mitophagy is essential for maintaining cardiac function during high fat diet-induced diabetic cardiomyopathy. Circ Res 124:1360–1371
28. Bravo-San Pedro JM, Kroemer G, Galluzzi L (2017) Autophagy and mitophagy in cardiovascular disease. Circ Res 120:1812–1824
29. Bonora M, Wieckowski MR, Sinclair DA, Kroemer G, Pinton P, Galluzzi L (2019) Targeting mitochondria for cardiovascular disorders: therapeutic potential and obstacles. Nat Rev Cardiol 16:33–55
30. Nishida Y, Arakawa S, Fujitani K, Yamaguchi H, Mizuta T, Kanaseki T, Komatsu M, Otsu K, Tsujimoto Y, Shimizu S (2009) Discovery of Atg5/Atg7-independent alternative macroautophagy. Nature 461:654–658
31. Kobayashi S, Liang Q (2015) Autophagy and mitophagy in diabetic cardiomyopathy. Biochim Biophys Acta 1852:252–261
32. Xu X, Kobayashi S, Chen K, Timm D, Volden P, Huang Y, Gulick J, Yue Z, Robbins J, Epstein PN et al (2013) Diminished autophagy limits cardiac injury in mouse models of type 1 diabetes. J Biol Chem 288:18077–18092
33. Lu W, Sun J, Yoon JS, Zhang Y, Zheng L, Murphy E, Mattson MP, Lenardo MJ (2016) Mitochondrial protein PGAM5 regulates mitophagic protection against cell necroptosis. PLoS One 11:e0147792
34. Hoshino A, Matoba S, Iwai-Kanai E, Nakamura H, Kimata M, Nakaoka M, Katamura M, Okawa Y, Ariyoshi M, Mita Y et al (2012) p53-TIGAR axis attenuates mitophagy to exacerbate cardiac damage after ischemia. J Mol Cell Cardiol 52:175–184
35. Kageyama Y, Hoshijima M, Seo K, Bedja D, Sysa-Shah P, Andrabi SA, Chen W, Hoke A, Dawson VL, Dawson TM et al (2014) Parkin-independent mitophagy requires Drp1 and maintains the integrity of mammalian heart and brain. EMBO J 33:2798–2813
36. Ikeda Y, Shirakabe A, Maejima Y, Zhai P, Sciarretta S, Toli J, Nomura M, Mihara K, Egashira K, Ohishi M et al (2015) Endogenous Drp1 mediates mitochondrial autophagy and protects the heart against energy stress. Circ Res 116:264–278
37. Cahill TJ, Leo V, Kelly M, Stockenhuber A, Kennedy NW, Bao L, Cereghetti GM, Harper AR, Czibik G, Liao C et al (2015) Resistance of dynamin-related protein 1 oligomers to disassembly impairs Mitophagy, resulting in myocardial inflammation and heart failure. J Biol Chem 290:25907–25919

38. Knowlton AA, Chen L, Malik ZA (2014) Heart failure and mitochondrial dysfunction: the role of mitochondrial fission/fusion abnormalities and new therapeutic strategies. J Cardiovasc Pharmacol 63:196–206
39. Dorn GW 2nd (2015) Mitochondrial dynamism and heart disease: changing shape and shaping change. EMBO Mol Med 7:865–877
40. Givvimani S, Pushpakumar S, Veeranki S, Tyagi SC (2014) Dysregulation of Mfn2 and Drp-1 proteins in heart failure. Can J Physiol Pharmacol 92:583–591
41. Chang JY, Yi HS, Kim HW, Shong M (2017) Dysregulation of mitophagy in carcinogenesis and tumor progression. Biochim Biophys Acta Bioenerg 1858:633–640
42. Chourasia AH, Tracy K, Frankenberger C, Boland ML, Sharifi MN, Drake LE, Sachleben JR, Asara JM, Locasale JW, Karczmar GS et al (2015) Mitophagy defects arising from BNip3 loss promote mammary tumor progression to metastasis. EMBO Rep 16:1145–1163
43. Liu J, Zhang C, Hu W, Feng Z (2018) Parkinson's disease-associated protein Parkin: an unusual player in cancer. Cancer Commun 38:40
44. Zhang C, Lin M, Wu R, Wang X, Yang B, Levine AJ, Hu W, Feng Z (2011) Parkin, a p53 target gene, mediates the role of p53 in glucose metabolism and the Warburg effect. Proc Natl Acad Sci U S A 108:16259–16264
45. Vara-Perez M, Felipe-Abrio B, Agostinis P (2019) Mitophagy in cancer: a tale of adaptation. Cell 8:493
46. Balamurugan K (2016) HIF-1 at the crossroads of hypoxia, inflammation, and cancer. Int J Cancer 138:1058–1066
47. Larsen SB, Hanss Z, Kruger R (2018) The genetic architecture of mitochondrial dysfunction in Parkinson's disease. Cell Tissue Res 373:21–37
48. Pickrell AM, Youle RJ (2015) The roles of PINK1, parkin, and mitochondrial fidelity in Parkinson's disease. Neuron 85:257–273
49. Chen J, Ren Y, Gui C, Zhao M, Wu X, Mao K, Li W, Zou F (2018) Phosphorylation of Parkin at serine 131 by p38 MAPK promotes mitochondrial dysfunction and neuronal death in mutant A53T alpha-synuclein model of Parkinson's disease. Cell Death Dis 9:700
50. Shaltouki A, Hsieh CH, Kim MJ, Wang X (2018) Alpha-synuclein delays mitophagy and targeting Miro rescues neuron loss in Parkinson's models. Acta Neuropathol 136:607–620
51. Bonifati V, Rizzu P, Squitieri F, Krieger E, Vanacore N, van Swieten JC, Brice A, van Duijn CM, Oostra B, Meco G et al (2003) DJ-1(PARK7), a novel gene for autosomal recessive, early onset parkinsonism. Neurol Sci 24:159–160
52. Krebiehl G, Ruckerbauer S, Burbulla LF, Kieper N, Maurer B, Waak J, Wolburg H, Gizatullina Z, Gellerich FN, Woitalla D et al (2010) Reduced basal autophagy and impaired mitochondrial dynamics due to loss of Parkinson's disease-associated protein DJ-1. PLoS One e9367:5
53. Joselin AP, Hewitt SJ, Callaghan SM, Kim RH, Chung YH, Mak TW, Shen J, Slack RS, Park DS (2012) ROS-dependent regulation of Parkin and DJ-1 localization during oxidative stress in neurons. Hum Mol Genet 21:4888–4903
54. Wang X, Winter D, Ashrafi G, Schlehe J, Wong YL, Selkoe D, Rice S, Steen J, LaVoie MJ, Schwarz TL (2011) PINK1 and Parkin target Miro for phosphorylation and degradation to arrest mitochondrial motility. Cell 147:893–906
55. Pareyson D, Saveri P, Sagnelli A, Piscosquito G (2015) Mitochondrial dynamics and inherited peripheral nerve diseases. Neurosci Lett 596:66–77
56. Rizzo F, Ronchi D, Salani S, Nizzardo M, Fortunato F, Bordoni A, Stuppia G, Del Bo R, Piga D, Fato R et al (2016) Selective mitochondrial depletion, apoptosis resistance, and increased mitophagy in human Charcot-Marie-tooth 2A motor neurons. Hum Mol Genet 25:4266–4281
57. Martin-Maestro P, Gargini R, Perry G, Avila J, Garcia-Escudero V (2016) PARK2 enhancement is able to compensate mitophagy alterations found in sporadic Alzheimer's disease. Hum Mol Genet 25:792–806
58. Cummins N, Tweedie A, Zuryn S, Bertran-Gonzalez J, Gotz J (2019) Disease-associated tau impairs mitophagy by inhibiting Parkin translocation to mitochondria. EMBO J 38: e99360
59. Rizzi L, Roriz-Cruz M (2018) Sirtuin 1 and Alzheimer's disease: an up-to-date review. Neuropeptides 71:54–60
60. Wang Y, Liu N, Lu B (2019) Mechanisms and roles of mitophagy in neurodegenerative diseases. CNS Neurosci Ther 25:859–875
61. Martinez-Vicente M, Talloczy Z, Wong E, Tang G, Koga H, Kaushik S, de Vries R, Arias E, Harris S, Sulzer D et al (2010) Cargo recognition failure is responsible for

inefficient autophagy in Huntington's disease. Nat Neurosci 13:567–576

62. Meyer H, Bug M, Bremer S (2012) Emerging functions of the VCP/p97 AAA-ATPase in the ubiquitin system. Nat Cell Biol 14:117–123
63. Guo X, Sun X, Hu D, Wang YJ, Fujioka H, Vyas R, Chakrapani S, Joshi AU, Luo Y, Mochly-Rosen D et al (2016) VCP recruitment to mitochondria causes mitophagy impairment and neurodegeneration in models of Huntington's disease. Nat Commun 7:12646
64. Guedes-Dias P, de Proenca J, Soares TR, Leitao-Rocha A, Pinho BR, Duchen MR, Oliveira JM (2015) HDAC6 inhibition induces mitochondrial fusion, autophagic flux and reduces diffuse mutant huntingtin in striatal neurons. Biochim Biophys Acta 1852:2484–2493
65. Guedes-Dias P, Oliveira JM (2013) Lysine deacetylases and mitochondrial dynamics in neurodegeneration. Biochim Biophys Acta 1832:1345–1359
66. Lee JY, Nagano Y, Taylor JP, Lim KL, Yao TP (2010) Disease-causing mutations in parkin impair mitochondrial ubiquitination, aggregation, and HDAC6-dependent mitophagy. J Cell Biol 189:671–679
67. Lee JY, Koga H, Kawaguchi Y, Tang W, Wong E, Gao YS, Pandey UB, Kaushik S, Tresse E, Lu J et al (2010) HDAC6 controls autophagosome maturation essential for ubiquitin-selective quality-control autophagy. EMBO J 29:969–980
68. Evans CS, Holzbaur ELF (2019) Autophagy and mitophagy in ALS. Neurobiol Dis 122:35–40
69. Rosen DR, Siddique T, Patterson D, Figlewicz DA, Sapp P, Hentati A, Donaldson D, Goto J, O'Regan JP, Deng HX et al (1993) Mutations in Cu/Zn superoxide dismutase gene are associated with familial amyotrophic lateral sclerosis. Nature 362:59–62
70. Manfredi G, Kawamata H (2016) Mitochondria and endoplasmic reticulum crosstalk in amyotrophic lateral sclerosis. Neurobiol Dis 90:35–42
71. Smith EF, Shaw PJ, De Vos KJ (2019) The role of mitochondria in amyotrophic lateral sclerosis. Neurosci Lett 710:132933
72. Moller A, Bauer CS, Cohen RN, Webster CP, De Vos KJ (2017) Amyotrophic lateral sclerosis-associated mutant SOD1 inhibits anterograde axonal transport of mitochondria by reducing Miro1 levels. Hum Mol Genet 26:4668–4679
73. Patergnani S, Pinton P (2015) Mitophagy and mitochondrial balance. Methods Mol Biol 1241:181–194
74. Dolman NJ, Chambers KM, Mandavilli B, Batchelor RH, Janes MS (2013) Tools and techniques to measure mitophagy using fluorescence microscopy. Autophagy 9:1653–1662
75. Klionsky DJ, Abdelmohsen K, Abe A, Abedin MJ, Abeliovich H, Acevedo Arozena A, Adachi H, Adams CM, Adams PD, Adeli K et al (2016) Guidelines for the use and interpretation of assays for monitoring autophagy (3rd edition). Autophagy 12:1–222
76. Katayama H, Kogure T, Mizushima N, Yoshimori T, Miyawaki A (2011) A sensitive and quantitative technique for detecting autophagic events based on lysosomal delivery. Chem Biol 18:1042–1052
77. Safiulina D, Kaasik A (2013) Energetic and dynamic: how mitochondria meet neuronal energy demands. PLoS Biol 11:e1001755
78. Yamano K, Wang C, Sarraf SA, Munch C, Kikuchi R, Noda NN, Hizukuri Y, Kanemaki MT, Harper W, Tanaka K et al (2018) Endosomal Rab cycles regulate Parkin-mediated mitophagy. eLife 7:e31326
79. Ding WX, Ni HM, Li M, Liao Y, Chen X, Stolz DB, Dorn GW 2nd, Yin XM (2010) Nix is critical to two distinct phases of mitophagy, reactive oxygen species-mediated autophagy induction and Parkin-ubiquitin-p62-mediated mitochondrial priming. J Biol Chem 285:27879–27890
80. Olenych SG, Claxton NS, Ottenberg GK, Davidson MW (2007) The fluorescent protein color palette. Curr Protoc Cell Biol Chapter 21:Unit 21.5
81. Patergnani S, Marchi S, Rimessi A, Bonora M, Giorgi C, Mehta KD, Pinton P (2013) PRKCB/protein kinase C, beta and the mitochondrial axis as key regulators of autophagy. Autophagy 9:1367–1385
82. Klionsky DJ, Abdalla FC, Abeliovich H, Abraham RT, Acevedo-Arozena A, Adeli K, Agholme L, Agnello M, Agostinis P, Aguirre-Ghiso JA et al (2012) Guidelines for the use and interpretation of assays for monitoring autophagy. Autophagy 8:445–544
83. Heo JM, Ordureau A, Paulo JA, Rinehart J, Harper JW (2015) The PINK1-PARKIN mitochondrial ubiquitylation pathway drives a program of OPTN/NDP52 recruitment and TBK1 activation to promote mitophagy. Mol Cell 60:7–20
84. Padman BS, Nguyen TN, Uoselis L, Skulsuppaisarn M, Nguyen LK, Lazarou M

(2019) LC3/GABARAPs drive ubiquitin-independent recruitment of Optineurin and NDP52 to amplify mitophagy. Nat Commun 10:408

85. Poole AC, Thomas RE, Yu S, Vincow ES, Pallanck L (2010) The mitochondrial fusion-promoting factor mitofusin is a substrate of the PINK1/parkin pathway. PLoS One e10054:5
86. Rakovic A, Grunewald A, Kottwitz J, Bruggemann N, Pramstaller PP, Lohmann K, Klein C (2011) Mutations in PINK1 and Parkin impair ubiquitination of Mitofusins in human fibroblasts. PLoS One 6:e16746
87. Tanaka A, Cleland MM, Xu S, Narendra DP, Suen DF, Karbowski M, Youle RJ (2010) Proteasome and p97 mediate mitophagy and degradation of mitofusins induced by Parkin. J Cell Biol 191:1367–1380
88. Patergnani S, Castellazzi M, Bonora M, Marchi S, Casetta I, Pugliatti M, Giorgi C, Granieri E, Pinton P (2018) Autophagy and mitophagy elements are increased in body fluids of multiple sclerosis-affected individuals. J Neurol Neurosurg Psychiatry 89:439–441
89. Castellazzi M, Patergnani S, Donadio M, Giorgi C, Bonora M, Fainardi E, Casetta I, Granieri E, Pugliatti M, Pinton P (2019) Correlation between auto/mitophagic processes and magnetic resonance imaging activity in multiple sclerosis patients. J Neuroinflammation 16:131
90. Castellazzi M, Patergnani S, Donadio M, Giorgi C, Bonora M, Bosi C, Brombo G, Pugliatti M, Seripa D, Zuliani G et al (2019) Autophagy and mitophagy biomarkers are reduced in sera of patients with Alzheimer's disease and mild cognitive impairment. Sci Rep 9:20009
91. Williams NC, O'Neill LAJ (2018) A role for the Krebs cycle intermediate citrate in metabolic reprogramming in innate immunity and inflammation. Front Immunol 9:141
92. Houten SM, Violante S, Ventura FV, Wanders RJ (2016) The biochemistry and physiology of mitochondrial fatty acid beta-oxidation and its genetic disorders. Annu Rev Physiol 78:23–44
93. Signes A, Fernandez-Vizarra E (2018) Assembly of mammalian oxidative phosphorylation complexes I-V and supercomplexes. Essays Biochem 62:255–270
94. Giorgi C, Marchi S, Pinton P (2018) The machineries, regulation and cellular functions of mitochondrial calcium. Nat Rev Mol Cell Biol 19:713–730
95. Giorgi C, Agnoletto C, Bononi A, Bonora M, De Marchi E, Marchi S, Missiroli S, Patergnani S, Poletti F, Rimessi A et al (2012) Mitochondrial calcium homeostasis as potential target for mitochondrial medicine. Mitochondrion 12:77–85
96. Marchi S, Bonora M, Patergnani S, Giorgi C, Pinton P (2017) Methods to assess mitochondrial morphology in mammalian cells mounting autophagic or mitophagic responses. Methods Enzymol 588:171–186
97. Jung C, Higgins CM, Xu Z (2000) Measuring the quantity and activity of mitochondrial electron transport chain complexes in tissues of central nervous system using blue native polyacrylamide gel electrophoresis. Anal Biochem 286:214–223
98. Bononi A, Yang H, Giorgi C, Patergnani S, Pellegrini L, Su M, Xie G, Signorato V, Pastorino S, Morris P et al (2017) Germline BAP1 mutations induce a Warburg effect. Cell Death Differ 24:1694–1704
99. Nicholas D, Proctor EA, Raval FM, Ip BC, Habib C, Ritou E, Grammatopoulos TN, Steenkamp D, Dooms H, Apovian CM et al (2017) Advances in the quantification of mitochondrial function in primary human immune cells through extracellular flux analysis. PLoS One 12:e0170975
100. Iuso A, Repp B, Biagosch C, Terrile C, Prokisch H (2017) Assessing mitochondrial bioenergetics in isolated mitochondria from various mouse tissues using seahorse XF96 analyzer. Methods Mol Biol 1567:217–230
101. De Biasi S, Simone AM, Bianchini E, Lo Tartaro D, Pecorini S, Nasi M, Patergnani S, Carnevale G, Gibellini L, Ferraro D et al (2019) Mitochondrial functionality and metabolism in T cells from progressive multiple sclerosis patients. Eur J Immunol 49:2204–2221
102. Menzies RA, Gold PH (1971) The turnover of mitochondria in a variety of tissues of young adult and aged rats. J Biol Chem 246:2425–2429
103. Kim TY, Wang D, Kim AK, Lau E, Lin AJ, Liem DA, Zhang J, Zong NC, Lam MP, Ping P (2012) Metabolic labeling reveals proteome dynamics of mouse mitochondria. Mol Cell Proteomics 11:1586–1594
104. Hernandez G, Thornton C, Stotland A, Lui D, Sin J, Ramil J, Magee N, Andres A, Quarato G, Carreira RS et al (2013)

MitoTimer: a novel tool for monitoring mitochondrial turnover. Autophagy 9:1852–1861

105. Zorova LD, Popkov VA, Plotnikov EY, Silachev DN, Pevzner IB, Jankauskas SS, Babenko VA, Zorov SD, Balakireva AV, Juhaszova M et al (2018) Mitochondrial membrane potential. Anal Biochem 552:50–59
106. Marchi S, Bittremieux M, Missiroli S, Morganti C, Patergnani S, Sbano L, Rimessi A, Kerkhofs M, Parys JB, Bultynck G et al (2017) Endoplasmic reticulum-mitochondria communication through Ca(2+) signaling: the importance of mitochondria-associated membranes (MAMs). Adv Exp Med Biol 997:49–67
107. Sakamuru S, Attene-Ramos MS, Xia M (2016) Mitochondrial membrane potential assay. Methods Mol Biol 1473:17–22
108. Scaduto RC Jr, Grotyohann LW (1999) Measurement of mitochondrial membrane potential using fluorescent rhodamine derivatives. Biophys J 76:469–477
109. Ward MW, Concannon CG, Whyte J, Walsh CM, Corley B, Prehn JH (2010) The amyloid precursor protein intracellular domain (AICD) disrupts actin dynamics and mitochondrial bioenergetics. J Neurochem 113:275–284